



Tmod2 Is a Regulator of Cocaine Responses through Control of Striatal and Cortical Excitability and Drug-Induced Plasticity

Arojit Mitra,¹ Sean P. Deats,¹ Price E. Dickson,¹ Jiuhe Zhu,² Justin Gardin,¹ Brian J. Nieman,³  R. Mark Henkelman,³  Nien-Pei Tsai,² Elissa J. Chesler,¹ Zhong-Wei Zhang,¹ and Vivek Kumar¹

¹The Jackson Laboratory, Bar Harbor, Maine 04609, ²Department of Molecular and Integrative Physiology, University of Illinois at Urbana-Champaign, Urbana, Illinois 61801, and ³Mouse Imaging Centre and Translational Medicine, Hospital for Sick Children; Ontario Institute for Cancer Research; Department of Medical Biophysics, University of Toronto, Toronto, Ontario M5T 3H7, Canada

Drugs of abuse induce neuroadaptations, including synaptic plasticity, that are critical for transition to addiction, and genes and pathways that regulate these neuroadaptations are potential therapeutic targets. *Tropomodulin 2* (*Tmod2*) is an actin-regulating gene that plays an important role in synapse maturation and dendritic arborization and has been implicated in substance abuse and intellectual disability in humans. Here, we mine the KOMP2 data and find that *Tmod2* knock-out mice show emotionality phenotypes that are predictive of addiction vulnerability. Detailed addiction phenotyping shows that *Tmod2* deletion does not affect the acute locomotor response to cocaine administration. However, sensitized locomotor responses are highly attenuated in these knock-outs, indicating perturbed drug-induced plasticity. In addition, *Tmod2* mutant animals do not self-administer cocaine indicating lack of hedonic responses to cocaine. Whole-brain MR imaging shows differences in brain volume across multiple regions, although transcriptomic experiments did not reveal perturbations in gene coexpression networks. Detailed electrophysiological characterization of *Tmod2* KO neurons showed increased spontaneous firing rate of early postnatal and adult cortical and striatal neurons. Cocaine-induced synaptic plasticity that is critical for sensitization is either missing or reciprocal in *Tmod2* KO nucleus accumbens shell medium spiny neurons, providing a mechanistic explanation of the cocaine response phenotypes. Combined, these data, collected from both males and females, provide compelling evidence that *Tmod2* is a major regulator of plasticity in the mesolimbic system and regulates the reinforcing and addictive properties of cocaine.

Key words: addiction; KOMP; MRI; striatal excitability; synaptic plasticity; transcriptomics

Significance Statement

We identify, characterize, and establish *tropomodulin 2* (*Tmod2*), an actin-regulating gene exclusively expressed in neurons, as an important regulator of addiction-related phenotypes. We show that *Tmod2*, knock-out mice (*Tmod2* KO) exhibit phenotypes that are predictive of addiction. In detailed addiction phenotyping, we find that the *Tmod2* regulates cocaine sensitization and self-administration. We explore the anatomical, transcriptional, and electrophysiological mechanisms of this regulation. Combined, these studies provide compelling evidence that *Tmod2* is critical for synaptic plasticity necessary for transition to addiction.

Received June 27, 2023; revised Feb. 12, 2024; accepted Feb. 24, 2024.

Author contributions: A.M., Z.-W.Z., and V.K. designed research; A.M., S.P.D., P.E.D., J.Z., and B.J.N. performed research; A.M., P.E.D., J.G., B.J.N., and V.K. analyzed data; A.M. and V.K. wrote the paper.

We thank the members of the Kumar laboratory for their valuable input to this work especially Brain Geuther and Kevin Seburn for proofreading the manuscript and suggesting the layout of the figures. We also thank members of Dr. Zhong-Wei lab including Dr. Guoqiang Hou for helping A.M. in setting up the electrophysiology rig for slice recordings. We thank Avery Lopez for her help with behavioral assay. We thank Delia Hartley for her help with animal husbandry. We thank the entire Knockout Mouse Project team at The Jackson Laboratory—Jacqui White, Steve A. Murray, Robert E. Braun, James Clark, Pamela Fraungruber, Rose Presby, Zachary Seavey, and

Catherine Witmeyer. We thank JAX Scientific Services, including the Genome Technologies Group, and the Center for Biometric Analysis for their valuable contribution. This work was supported by the National Institute on Drug Abuse (NIDA) grant the National Institutes of Health NIDA U01DA041668, U01DA051235, and R33DA050837 and the Brain and Behavioral Foundation Young Investigator Award to V.K. and 5P50DA039841 to E.J.C.

The authors declare no competing financial interests.

Correspondence should be addressed to Vivek Kumar at vivek.kumar@jax.org.

<https://doi.org/10.1523/JNEUROSCI.1389-23.2024>

Copyright © 2024 the authors

Introduction

Multiple lines of evidence suggest that enduring functional and structural plasticity in reward-related brain regions is critical for transition to addiction (Grueter et al., 2012; Rothenfluh and Cowan, 2013). Although the entire brain reward circuit is vulnerable to drug-induced functional and structural remodeling, it is relatively well characterized in the nucleus accumbens (Volkow and Morales, 2015). Functional plasticity broadly refers to changes in intrinsic and synaptic properties of existing synapses, whereas structural plasticity includes morphological changes such as dendritic spine class and density alterations (Miller et al., 2012). Drug-induced synaptic plasticity in the nucleus accumbens is thought to play a key role in the development and maintenance of addiction, as well as in the susceptibility to relapse (Russo et al., 2010; Lüscher and Malenka, 2011; Wolf, 2016; Volkow et al., 2019). Drug-induced plasticity in the nucleus accumbens includes changes in intrinsic properties such as firing rate depression or synaptic changes through long-term potentiation (LTP), long-term depression (LTD), or metaplasticity. Different classes of drugs can induce different forms of synaptic plasticity in the nucleus accumbens through involvement of various neurotransmitters, receptors, signaling pathways, and epigenetic factors. For instance, cocaine can induce LTP of glutamatergic synapses on medium spiny neurons in a dose-dependent and experience-dependent manner (Kourrich et al., 2007). Interestingly, NMDA-dependent LTD in the nucleus accumbens (Kasanez et al., 2010) and mGluR2/3-dependent LTD in the prelimbic cortex (Kasanez et al., 2013) are abolished in cocaine-addicted-like rats while being maintained in cocaine nonaddicted-like rats. Similarly, opioids can induce LTP of glutamatergic synapses on medium spiny neurons by activating μ -opioid receptors and inhibiting GABAergic interneurons (Turner et al., 2018). Opioids can also induce LTD of glutamatergic synapses by activating δ -opioid receptors and enhancing endocannabinoid signaling (Turner et al., 2018). Alcohol can also induce LTP of glutamatergic synapses on medium spiny neurons by increasing the activity of calcium/calmodulin-dependent protein kinase II (CaMKII) and enhancing AMPA receptor trafficking and can be prevented by NMDA receptor antagonists or by inhibiting CaMKII (van Huijstee and Mansvelder, 2015). Alcohol can also induce LTD of glutamatergic synapses by activating adenosine A1 receptors and reducing cAMP levels (van Huijstee and Mansvelder, 2015). Thus, although the circuitry that regulates addiction properties is conserved, the mechanism through which it is regulated can vary.

Along with functional plasticity, repeated drug administration is also thought to facilitate structural plasticity in the mesolimbic circuit. Repeated administration of psychostimulants correlates with increased spine density and dendritic complexity in the nucleus accumbens, ventral tegmental area, and prefrontal cortex neurons (Russo et al., 2010). Dendritic spines are actin-rich protrusions of the neural plasma membrane that are the major postsynaptic sites of excitatory signaling in the brain and subcellular substrate of synaptic and structural plasticity. Perturbations in actin-assembly (Feng et al., 2000; Deller et al., 2003; Wu et al., 2008; Kim et al., 2009; Lin et al., 2010), actin-capping (Cox et al., 2003; Offenhauser et al., 2006), actin-disassociating (Furukawa et al., 1997; Star et al., 2002), actin-nucleating (Soderling et al., 2007; Kumar et al., 2013), and actin-ADP/ATP exchange (Pilo-Boyl et al., 2007) proteins affects synaptic and structural plasticity. Previous studies have implicated actin dysregulation in morphine (Li et al., 2015), cocaine (Toda et al., 2006), methamphetamine (Young et al., 2015), alcohol (Ojelade et al., 2015), and nicotine

(Ryder, 1994; Gu et al., 2013) addiction. Generally, psychostimulant administration correlates with increases in spine numbers, spine complexity, and spine maturity (Norrholm et al., 2003; Robinson and Kolb, 2004; Miller et al., 2012). These structural changes occur through actin-mediated rearrangements (Star et al., 2002; Soderling et al., 2007; Kumar et al., 2013). Consistent with these observations, nonmuscle myosin IIB inhibitor, which mitigates spine maturation by inhibiting cross-linking and treadmilling of F-actin, has been shown effective in preventing relapse to methamphetamine (Young et al., 2016). Our previous study demonstrated that a point mutation in actin-regulating cytoplasmic FMRP-interacting protein-2 (*Cyfp2*) in mice decreases both acute and sensitized cocaine responses (Kumar et al., 2013). However, a causal link between structural changes and behavioral effects of repeated exposure to drugs remains controversial (Rothenfluh and Cowan, 2013). Genetic or pharmacological perturbations of factors that are known to regulate structural plasticity, such as kalirin-7, myocyte enhancer factor-2, and cyclin-dependent kinase-5, fail to attenuate behavioral locomotor sensitization in mice (Norrholm et al., 2003; Benavides et al., 2007; Pulipparacharuvi et al., 2008; Kiraly et al., 2010). Thus, the possibility has been raised that structural plasticity in transition to addiction is an “epiphenomenon” (Rothenfluh and Cowan, 2013).

The neuron-specific, tropomyosin-dependent pointed end-capping protein tropomodulin-2 (TMOD2) stabilizes an actin filament by preventing depolymerization and elongation (Weber et al., 1999). Four isoforms of tropomodulin (*Tmod1–4*) are expressed with tissue specificity in mice. *Tmod1* and *Tmod3* are ubiquitously expressed, whereas *Tmod4* and *Tmod2* are restricted to muscles and neurons, respectively (Fischer and Fowler, 2003). Previous studies have established a role for TMOD2 in dendritic arborization (Omotade et al., 2018) and spine maturation (Gray et al., 2016). During development, its expression coincides with generation, migration, and extension of cerebrum and cerebellum neurons during the prenatal period (Mark and Sussman, 1994; Watakabe et al., 1996). In addition to the pointed end capping of the actin filament, an in vitro protein interaction study shows actin-monomer binding and strong actin-nucleation activity by TMOD2 (Yamashiro et al., 2010). Zoghbi and colleagues were the first to develop and characterize the *Tmod2* knock-out mice and elegantly showed that its loss leads to novelty-induced hyperactivity, memory deficits in a fear-conditioning task, and enhanced long-term potentiation at hippocampal synapses (Cox et al., 2003). Congruently, recent human GWAS studies have shown that *Tmod2* haplotypes are associated with intellectual and cognitive impairments (Davies et al., 2018; Hill et al., 2019). In human candidate gene studies for addiction traits, Gelernter and colleagues showed that *Tmod2* is associated with drug-dependent risk-taking behavior and proposed TMOD2-mediated remodeling of brain areas as a regulator of risky sexual behavior and drug intake (Polimanti et al., 2017). In several transcriptomic and proteomic studies, *Tmod2* mRNA and protein levels are differentially modulated following repeated methamphetamine (Iwazaki et al., 2006; Zhang et al., 2013; Zhu et al., 2016), alcohol (Lesscher et al., 2012), cocaine (Oliver et al., 2018), or morphine (Tapocik et al., 2013) administration in animal models. These studies led a meta-analysis to suggest that *Tmod2* is an addiction candidate gene (Li et al., 2008). However, to date, there has not been a study that directly investigates a causal role of *Tmod2* in addiction phenotypes and provides mechanistic insights into its function in the reward circuit.

Based on recent human genetic data and our mining of the Knockout Mouse Project (KOMP) behavior phenotype data,

we hypothesized that *Tmod2* is a regulator of addiction-related phenotypes. To test this, we carried out detailed addiction phenotype characterization for cocaine responses and find that sensitized response and intravenous self-administration (IVSA) acquisition are diminished in *Tmod2* knock-out mice. Imaging and genomic data show reduced brain size but no major perturbances in gene coexpression networks, respectively. Finally, a detailed characterization of the intrinsic properties of cortical and striatal neurons at postnatal and adult stages show enhanced excitability. Synaptic events that are hallmarks of cocaine-induced synaptic plasticity in the nucleus accumbens medium spiny neurons are missing in the knock-outs. Together, our data provide compelling evidence that the actin-regulating gene *Tmod2* plays a critical role in cocaine-induced behavioral adaptations that are critical for transition to addiction.

Materials and Methods

Animals and drugs

Tropomodulin 2 (*Tmod2*^{-/-}) knock-out mice, B6N(Cg)-*Tmod2*^{tm1b(KOMP)Wtsi/2J} (JR# 024939; referred to as *Tmod2* KO in text or KO in figures) with a LacZ reporter gene, and C57BL/6NJ (JR# 005304; control referred to as WT) mice were obtained from The Jackson Laboratory. Both male and female mice were used for experiments. Mice were bred for at least two generations in an in-house colony before experimentation. Animal handling and experimental procedures were approved by the Institutional Animal Care and Use Committees at The Jackson Laboratory. Cocaine hydrochloride (CAS #53-21-4, Sigma-Aldrich) was dissolved in 0.9% NaCl (vehicle) and was administered intraperitoneally.

Data mining from KOMP repository

Data generated by The Jackson Laboratory's KOMP phenotyping pipeline on *Tmod2* KO mice were harvested from the International Mouse Phenotyping Consortium website and is publically available at <http://www.mousephenotype.org/data/genes/MGI:1355335#section-associations>. Details of the phenotyping pipeline, behavioral assays, and parameters are available at <http://www.mousephenotype.org/impress/procedures/7>. Habituation ratio is calculated as the ratio of the distance traveled in the first and last 5 min of the open field test.

Locomotor response to acute injection of cocaine

All testing was carried out between Zeitgeber time 3 and 11 (ZT 3–11). Mice were habituated to handling and testing room conditions prior to behavioral assays. Mice (10 weeks old) were brought into the testing room and habituated to the open field testing room for 1 h with white noise (75 ± 2 decibels), before introducing them to the open field. Locomotor activity was recorded using an overhead camera and LimeLight software (Actimetrics) before and after the injections. One single dose of low (10 mg/kg) or high (20 mg/kg) dose of cocaine was injected, and the locomotor activity was recorded for 1 h (Kumar et al., 2011).

Locomotor sensitization

Following 1 h habituation to the testing room, mice (10 weeks old) were introduced in an open field arena, and locomotor activities before and after the saline or cocaine injections were recorded. Mice received saline for 4 d and cocaine (15 mg/kg) for the next 6 d followed by one saline injection on Day 11. A same-dose cocaine challenge on Day 17 and an additional challenge on Day 24 were given (see timeline in Fig. 2D; Kumar et al., 2011). For intersession habituation over 4 d, it is calculated as Day 4 activity / (Day 1 activity + Day 4 activity). For intrasession habituation in a 20 min session, it is final 5 min activity / (initial 5 min activity + final 5 min activity). A score near 0.5 indicates no change, near 0 indicates habituation, and near 1 indicates increased activity (Bolivar, 2009).

Intravenous self-administration assay

The cocaine IVSA testing procedure and chambers have been described in detail previously (Dickson et al., 2011). Mice began cocaine IVSA

testing on a fixed-ratio 1 schedule at a dose of 1.0 mg/kg/infusion. Mice were tested in 2 h sessions at the same time daily 7 d per week throughout the experiment. Acquisition criteria were defined as (1) ≥10 infusions per session on three consecutive or nonconsecutive sessions followed by (2) two consecutive sessions during which the number of infusions was ≥10, did not vary by >20%, and ≥70% of lever presses were on the active lever.

Sucrose preference

Mice were singly housed for this protocol in a cage with the metal roof lid having inserts for 2–3 bottles and access to *ad libitum* chow. Baseline water consumption was assessed by providing water in two bottles for 4 consecutive days and measuring bottle weight in 24 h interval. At the end of the fourth day, one of the bottles is filled with freshly prepared 4% sucrose solution, and consumption was assessed for the next 4 d. The position of the bottles was changed daily to avoid any physical preference or side bias toward the bottle. The bedding below the sipper bottles was monitored daily to account for spillage. If the bedding was found moist or wet with an unusual quantity of consumption for a day, the intake data were not included in the analysis. Preference is calculated as the percentage of the sucrose consumed over the total volume of fluid intake on Day 8 (Eagle et al., 2015).

Operant conditioning for food reward

Nine-week-old mice were subjected to mild food restriction to maintain 80–90% of *ad libitum* body weight (BW) during the entire 15 d of the protocol. Mice were habituated to the operant chamber (Med Associates) for 30 min for 2–3 d with house light and fan on and levers retracted. Following habituation, levers were made accessible, and the active lever press was associated with a delivery of one (FR1) 15 mg sucrose pellet (#S05550; Bio-Serv) as a reward and a time-out period of 20 s during which the house light is switched off. Inactive lever press was not associated with any reward or observable stimuli. Daily 1 h sessions were provided at the same time of the day, for 10 d. The total number of sucrose pellets earned and the number of active and inactive lever press were recorded and statistically compared between *Tmod2* KO and WT. On the subsequent 5 d (Day 11–15), an extinction paradigm was introduced where active lever press yielded no reward and the house light stayed on for the entirety of the session. On Day 16, a reinstatement session was provided, with conditions similar to the acquisition phase during Day 1–10.

Magnetic resonance imaging

Ten-week-old *Tmod2* KO ($n = 15$) and WT ($n = 19$) were deeply anesthetized and transcardially perfused with 30 ml, 1× PBS with 1 μl/ml heparin and 2 mM ProHance (Bracco Diagnostics) at room temperature, at a flow rate of 1 ml/min. Fixation, storage, and imaging procedures have been described in detail previously (de Guzman et al., 2016; Spencer Noakes et al., 2017). For this study, T₂-weighted RARE images were acquired on a 7-T scanner (Varian/Agilent) with imaging parameters: TE_{eff} = 30 ms, TR = 350 ms, six echoes, four averages, 40 μm resolution, and 13 h scan time. The resulting images were analyzed using an automated registration pipeline (Friedel et al., 2014) in conjunction with pre-defined structural atlases (Dorr et al., 2008). The resulting images obtained were analyzed for total brain, total gray matter, and total white matter volume differences. Regional differences in structure were assessed through two different methods. In the first, we measured (absolute) volumes for each structure to evaluate the differences between genotypes, fitting with a linear model with sex, genotype, and sex–genotype interaction coefficients. Significance was determined after correction for multiple comparisons through the false discovery rate (and expressed as q values; Benjamini and Hochberg, 1995). In a second analysis, individual structure volumes were normalized to total brain volume so that each structure was evaluated as a percentage of total brain volume. The second approach accounts for a significant amount of the biological variability between mice (Lerch et al., 2012).

Bulk RNA sequencing

Naive, 10-week-old *Tmod2* KO ($n = 3$) and WT ($n = 3$) mice were killed by cervical dislocation, and the brains were harvested rapidly in an ice-

cold 1× PBS. One-mm-thick coronal sections were obtained using a stainless steel brain matrix (Stoelting), and punches were taken from the primary and secondary motor cortices and striatum. The punches were immediately transferred in 1.5 ml tubes containing 250 μ l of RNAlater (#AM7020, Invitrogen) and stored at 4°C, overnight. Next day, these tubes were transferred to –80°C freezer for long-term storage. Tissues were lysed and homogenized with a TRIzol reagent (Ambion), and then RNA was isolated using the miRNeasy Mini kit (Qiagen), according to manufacturers' protocols, including the optional DNase digest step. Sample concentration and quality were assessed using the NanoDrop 2000 spectrophotometer (Thermo Fisher Scientific) and the RNA 6000 Nano LabChip assay (Agilent Technologies). Libraries were prepared by the Genome Technologies core facility at The Jackson Laboratory using the KAPA mRNA HyperPrep kit (KAPA Biosystems), according to the manufacturer's instructions. Briefly, the protocol entails isolation of poly(A) containing mRNA using oligo-dT magnetic beads, RNA fragmentation, first and second strand cDNA synthesis, ligation of Illumina-specific adapters containing a unique barcode sequence for each library, and PCR amplification. Libraries were checked for quality and concentration using the D5000 ScreenTape assay (Agilent Technologies) and quantitative PCR (KAPA Biosystems), according to the manufacturers' instructions. For sequencing, libraries were pooled and sequenced by the Genome Technologies core facility at The Jackson Laboratory, 75 bp single-end on the NextSeq 500 (Illumina) using NextSeq High Output Kit v2 reagents (Illumina).

Electrophysiology

Microelectrode array (MEA) recordings on the primary cortical neuron culture. Primary cortical neuron cultures were made from mice P0–P1 as described previously (Tsai et al., 2012). Briefly, pups at P0–P1 ($n = 4$, *Tmod2* KO; $n = 6$, WT) were anesthetized on a cold metallic block placed on a bed of ice. Brains were taken out, and the entire cortical region was microdissected in an aseptic environment (a biochemical hood). Cortical tissues were immediately transferred to ice-cold Hibernate AB complete media (BrainBits) and were shipped to collaborators at the University of Illinois at Urbana-Champaign, Urbana, IL, USA. Details of cell dissociation, maintenance on MEA plates, recordings, and parameters analyzed and compared were described previously (Jewett et al., 2018). Briefly, on DIV 15, MEA plates were placed inside the recording chamber with inbuilt humidifier, and access to 5% CO₂ at 37°C. A 15 min baseline recording was obtained before the application of pharmacological agents such as the GABA-A receptor blocker picrotoxin (PTX) and the AMPA receptor antagonist NBQX. For analysis, a 10 min baseline spiking activity before drug application was compared with a 10 min response window following 5 min of drug application (Fig. 4B). Fold change in spontaneous spike rate, burst number, and synchrony index is a ratio of response and baseline periods. Fold change of 1 represents no change, >1 represents the response value of the parameter that was more than the baseline, and <1 represents a decrease in the response value.

Intrinsic properties of cortical and striatal neurons. Mice were deeply anesthetized using 4% tribromoethanol (800 mg/kg) and decapitated, and the brain was quickly dissected out in ice-cold solution containing the following (in mM): 210 sucrose, 26 NaHCO₃, 10 glucose, 3 KCl, 4 MgCl₂, and 1 CaCl₂ aerated with 95% O₂ and 5% CO₂. Using a vibratome (Leica VT1200), 250 μ m brain slices from naive, 8-week-old *Tmod2* KO ($n = 6$) and WT ($n = 6$) mice were obtained containing the prelimbic area (coronal sections) of the medial prefrontal cortex or accumbens shell (sagittal sections). Slices were then transferred to a holding chamber with artificial cerebrospinal fluid (ACSF) at room temperature containing the following (in mM): 124 NaCl, 3.0 KCl, 1.5 CaCl₂, 1.3 MgCl₂, 1.0 NaH₂PO₄, 26 NaHCO₃, and 20 glucose, saturated with 95% O₂ and 5% CO₂ at room temperature (21–24°C). Slices were incubated for at least 1 h for neurons to recover and equilibrate to the ACSF, before performing the whole-cell recordings. For recordings, slices were transferred to a submersion-type chamber attached to a microscope and were continuously perfused with ACSF saturated with 95% O₂ and 5% CO₂ at 30–32°C. The pyramidal cells of the prelimbic cortex and medium spiny neurons in the accumbens shell were identified using a 40× objective. The

medium spiny neurons were additionally screened by their low resting membrane potential of –75 mV or lower. Whole-cell recordings were obtained from neuron cell bodies using a MultiClamp 700B amplifier (Molecular Devices) and glass pipette containing the following (in mM): 120 K-gluconate, 20 KCl, 10 HEPES, 0.2 EGTA, 2 MgCl₂, and ATP/GTP, pH 7.2–7.3. Series resistance was fully compensated in current-clamp mode. All the protocols were made and executed through the AxoGraph X software (AxoGraph Scientific). Data were filtered at 4 kHz and digitized at 20 kHz. Data analysis was performed using AxoGraph X.

The intrinsic properties of neurons were analyzed using the methods described previously (Zhang, 2004; Zhang and Arsenault, 2005). Resting membrane potentials were measured within 20 s of break-in. Input resistance, time constant, and whole-cell capacitance were calculated from voltage responses to 700 ms current steps of –40 pA. To compensate for changes in the resting membrane potential, cells in the prelimbic cortex and accumbens shell were held at –70 and –80 mV, respectively, between current steps.

Synaptic properties of striatal neurons. Nine-week-old *Tmod2* KO ($n = 6$) and WT ($n = 6$) mice were injected either with saline ($n = 6$, three from each strain) or cocaine (15 mg/kg; $n = 6$, three from each strain), once per day for 5 d. Following injections, mice were transferred to a new cage to facilitate locomotor sensitization (Badiani and Robinson, 2004). After 3–8 d of abstinence, mice were killed, and sagittal brain sections containing accumbens shell regions were obtained as mentioned above. The recording ACSF contains 0.5 μ M tetrodotoxin in addition to the ingredients mentioned earlier. A nonpotassium, cesium (Cs)-based pipette solution was used containing the following (in mM): 117 Cs-gluconate, 20.0 HEPES, 0.4 EGTA, 2.8 NaCl, 5.0 tetraethylammonium chloride, and 4.0 QX-314, pH 7.2–7.3. Recordings were performed in voltage-clamp mode, and cells were held at –60 mV for recording miniature excitatory postsynaptic current (mEPSC) and thereafter, at +5 mV for recording miniature inhibitory postsynaptic current (mIPSC). The amplitude, frequency, rise, and decay time of mEPSCs and mIPSCs were analyzed using AxoGraph X as described previously (Zhang et al., 2014).

Results

Addiction-predictive behavior assessment using data in KOMP repository

A large body of literature suggests common underlying neurobiological pathways between addiction traits and other behavioral traits. Behavioral traits, such as anxiety, novelty seeking, stress, and impulsivity, are predictive of alcohol- and drug-related phenotypes in humans and rodents. In humans, epidemiological studies show comorbidity between addiction phenotypes and sensation seeking, impulsivity, and anxiety (Ball et al., 1998; Franques et al., 2003; Brady et al., 2013). These human studies are consistent with studies in experimental animals indicating that sensation seeking, novelty preference, and impulsivity predict psychostimulant self-administration (Molander et al., 2011; Dickson et al., 2015). In genetically diverse outbred rat studies, novelty preference (Belin et al., 2011), anxiousness (Dilleen et al., 2012), and impulsivity, but not novelty-induced hyperlocomotor activity (Belin et al., 2008), predict vulnerability to cocaine addiction-like behavior in rats.

Since KOMP uses metadata splits that can create imbalanced classes of controls and mutants, we reanalyzed the existing data using local controls. We analyzed the *Tmod2* phenotype data present in the public domain through the KOMP repository. Data from *Tmod2* knock-out ($n = 16$) and WT mice (C57BL/6NJ; $n = 68$ –92) that were tested concurrently ± 3 d were used for all the analyses. We specifically analyzed results obtained from open-field assay (OFA), light/dark box assay (LD), hole-board assay (HB), paired-pulse inhibition test (PPI), grip

strength, rotarod test (RR), sleep-wake percentage, body composition, and clinical blood chemistry parameters (Fig. 1-1).

Hyperactivity and low anxiety in novel environment

Open-field behavior measures general locomotor activity, exploratory drive, anxiety-related behavior, and habituation learning. The mice were allowed to explore the open-field arena, undisturbed, for 20 min, and the activity was statistically compared in four, 5 min bins (Fig. 1A1). *Tmod2* KO mice exhibit

general hyperactivity that persisted for 20 min with a sign of habituation as seen by the bin-to-bin decline in distance traveled in 20 min (Fig. 2A). *Tmod2* KO mice show persistent hyperactivity compared with WT with increased number of breaks in all four, 5 min bins [Fig. 1A1; genotype, $F_{(1,328)} = 180$, $p < 0.0001$; time-bins, $F_{(3,328)} = 22.43$, $p < 0.0001$; genotype \times time-bins, $F_{(3,328)} = 10.05$, $p < 0.0001$; Fig. 2A]. Consequently, the total time spent mobile was also significantly elevated in *Tmod2* KO (Fig. 1A5; $t = 7.973$; $p < 0.0001$). *Tmod2* KO mice spend more

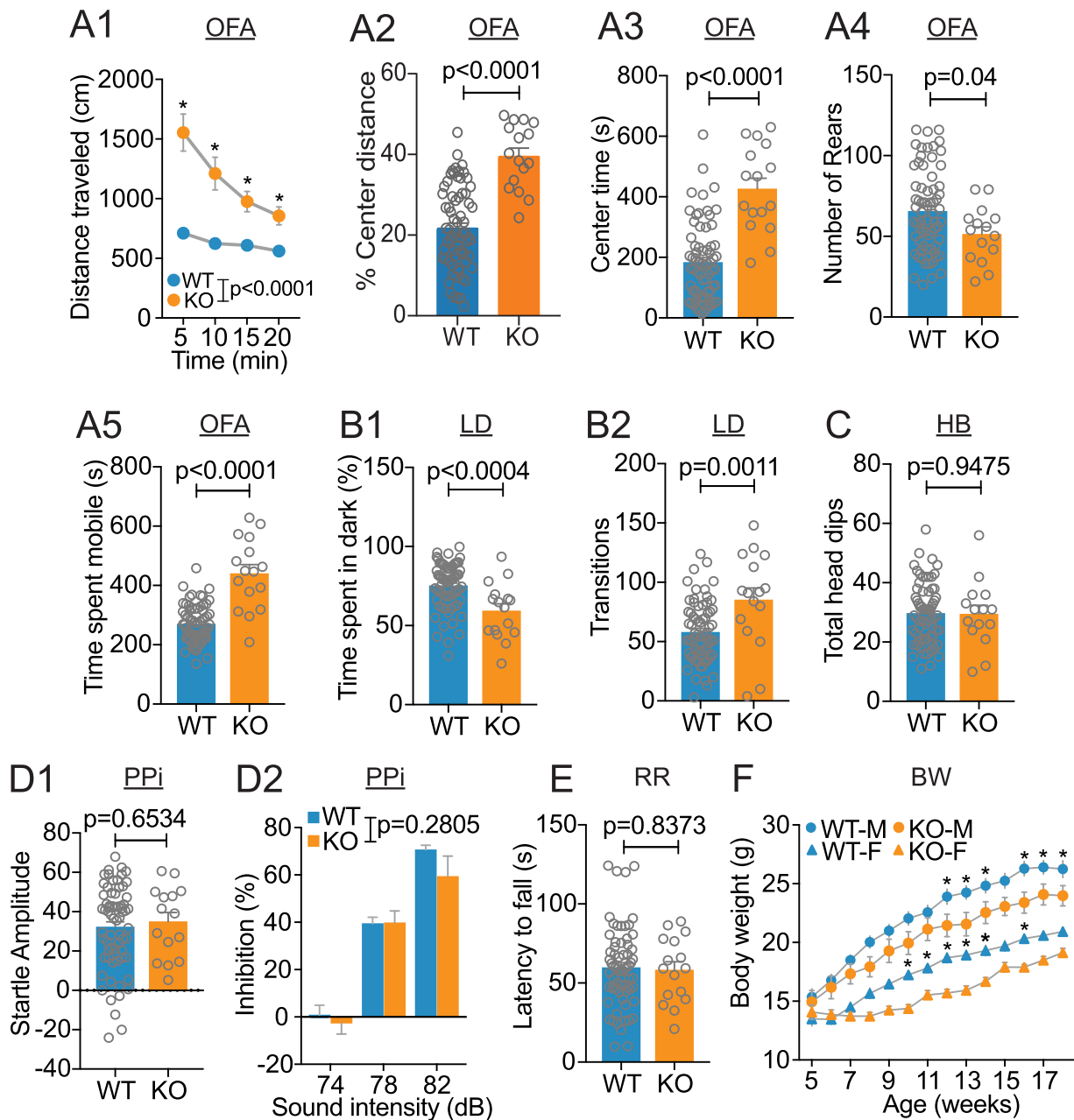


Figure 1. Behavioral characterization of *Tmod2* KO using publicly available data in KOMP repository shows specific deficits in hyperactivity and anxiety phenotypes. **A1–A5**, Open-field assay results; (**A1**) distance traveled in a 20 min exposure to standard open-field arena in four, 5 min [*Bonferroni's multiple comparison post hoc test detected significant differences ($p < 0.0001$) between WT and KO mice]; (**A2**) percentage of distance traveled in the center and (**A3**) mean total time spent in the center; (**A4**) number of rear postures attained; (**A5**) total time spent mobile. **B1, B2**, LD box results; (**B1**) time spent in the dark side of the LD; (**B2**) number of transitions between light and dark regions. **C**, 20 min exposure to HB. **D1–D2**, Prepulse inhibition assay results; (**D1**) startle amplitude and (**D2**) percentage inhibition of reaction to a subsequent stronger acoustic stimulus. **E**, Rotarod performance test. **F**, Only those mice that have BW data for all the 14 weeks were taken for analysis (WT, $n = 30$, 15 males, 15 females; KO, $n = 16$, 8 males, 8 females). BW growth curve (*significantly different from same-sex *Tmod2* KO, $p < 0.05$). Error bar represents SEM. OFA, open-field assay; LD, light/dark box; HB, hole-board assay; PPI, paired-pulse inhibition; RR, rotarod test; BW, body weight growth curve. All raw data retrieved from KOMP pipeline is provided as table in Extended Data Figure 1-1.

time in the center (Fig. 1A3; $t = 6.662$; $p < 0.0001$) and exhibit increased percent locomotor activity in the center of the open-field arena representing lower anxiety levels compared with WT (Fig. 1A2; $t = 10.1$; $p < 0.0001$). Rearing, a risk assessment and investigative behavior (Lever et al., 2006), was reduced in KOs (Fig. 1A4; $t = 2.055$; $p = 0.0431$). Therefore, the behavioral assessment of *Tmod2* KOs in an open field suggests a novelty-induced locomotor activity with decreased anxiety levels, intact habituation learning, and diminished risk assessment or an increased propensity for risk-taking behavior.

Low anxiety and risk-taking behavior toward aversive context

Behavioral assessment was carried out in a standard light/dark box with two zones with different light intensities. A brightly lit area is aversive and mice prefer the dark side. Exploration of the light side, as measured by the amount of time in the dark compared with the light side and the number of transitions between the two sides, is a form of risk-taking and anxiety behavior (Hascoët et al., 2001). *Tmod2* KO spent significantly less time in the dark compared with WT (Fig. 1B1; $t = 3.72$; $p = 0.0004$) and had a greater number of transitions between the light and dark zones (Fig. 1B2; $t = 3.382$; $p = 0.0011$). This assay provides complementary evidence of the novelty-induced hyperactivity, increased risk-taking, and low anxiety behavior in *Tmod2* KO that was seen in the open field assay.

Intact general exploratory behavior, sensory motor gating, and motor coordination and learning

Even though *Tmod2* KO appears to be hyperactive and less anxious in a novel environment, other parameters such as general exploration, sensory motor gating, and motor learning are intact. General exploration is measured using the hole-board apparatus that consists of a floor with multiple holes (16 in total) and elicits an exploratory head-dipping exploratory behavior. Total head dips in a 20 min window were found to be comparable in *Tmod2* KO and WT (Fig. 1C; $t = 0.06607$; $p = 0.9475$), indicating no deficits in general exploration behavior in *Tmod2* KO.

Sensory motor gating is measured using the PPI protocol. This behavioral assay was carried out in a sound-attenuated chamber. Startle response amplitude (Fig. 1D1; $t = 0.4508$; $p = 0.6534$) and percent inhibition to an increasing levels of prepulse sound prior to aversive sound stimuli were comparable in KOs and WT [Fig. 1D2; genotype, $F_{(1,240)} = 1.17$, $p = 0.2805$; sound intensity, $F_{(2,240)} = 80.02$, $p < 0.0001$; genotype \times sound intensity, $F_{(2,240)} = 0.6452$, $p = 0.5255$], indicating unperturbed sensory motor gating in *Tmod2* KO. The effects of *Tmod2* deletion on motor learning and coordination were assessed using the RR. In this test, motor learning is tested by calculating mean latency to fall in five consecutive trials on an accelerating cylindrical rod. *Tmod2* KO mice show no deficits in motor learning tasks, and their performance is comparable to their WT counterparts (Fig. 1E; $t = 0.206$; $p = 0.8373$).

Decreased BW that is slightly biased toward loss of lean mass

The KOMP phenotyping pipeline also collects weekly measurements of BW between the 5th and 18th weeks of age. *Tmod2* KO males and females show a significant decrease in BW relative to WT, which is more pronounced in late adulthood (10–12 weeks of age) [Fig. 1F; genotype, $F_{(1,42)} = 11.59$, $p = 0.001$; age \times genotype, $F_{(13,546)} = 10.38$, $p < 0.0001$; age \times sex, $F_{(13,546)} = 19.67$, $p < 0.0001$; genotype \times sex, $F_{(1,42)} = 0.001$, $p = 0.9741$]. Further exploration of body composition data from microCT scans revealed an increased lean body mass (Fig. 2E; $t = 2.437$; $p = 0.017$), suggestive of

decreased fat mass (Fig. 2F; $t = 1.719$; $p = 0.0893$) and a significant reduction in body length (Fig. 2D; $t = 4.43$; $p < 0.0001$) in *Tmod2* KO. Therefore, an age-dependent decrease in BW in *Tmod2* KO is due to a modified lean to fat mass ratio and hindered overall body growth or a combination of both. These data indicate that the *Tmod2* KO mice are ~22–28% smaller starting at 10–11 weeks of age. Clinical blood chemistry analysis detected an elevated alkaline phosphatase level (Fig. 2G; $t = 3.268$; $p = 0.009$) and decreased blood glucose levels in *Tmod2* KO mice (Fig. 2H; $t = 3.403$; $p = 0.001$). Total protein (Fig. 2I; $t = 1.857$; $p > 0.05$) and urea levels (Fig. 2J; $t = 2.377$; $p = 0.04$) are comparable in WT and *Tmod2* KO mice representing no overt kidney phenotype. Although smaller, these mice had no overt phenotype(s) and did not show any signs of illness or poor health. Combined, KOMP data demonstrate specific behavior signatures in *Tmod2* KO that have been shown previously to be predictive of addiction (Molander et al., 2011; Dickson et al., 2015), while several other parameters were found unchanged when compared with WT counterparts (Fig. 2B,C,F,I,J).

Comprehensive phenotyping for addiction-relevant behavior

Based on KOMP results, we generated a *Tmod2* KO colony and carried out addiction phenotyping. Prior to any behavioral analysis, we confirmed that TMOD2 was absent through Western blot analysis. The results confirmed the absence of TMOD2 protein in the mutant's cortical punches (Fig. 3A). In addition, later genomic analysis showed reduced levels of the *Tmod2* transcript (Fig. 4D).

Unaffected acute response to low and high doses of cocaine

Separate groups of WT and KO mice were acutely injected with cocaine (10 or 20 mg/kg), and their locomotor response was analyzed 30 min before and 1 h following injections (Fig. 3B,C). For statistical comparison, the net locomotor response was calculated by subtracting the total locomotor activity in a 30 min period following cocaine injections with the locomotor activity during 30 min baseline. The net locomotor response was comparable between mutants and WT for both doses of cocaine indicating that the neural circuits that evoke acute drug-induced locomotor response were intact in *Tmod2* KO [Fig. 3D; genotype, $F_{(1,89)} = 0.509$, $p = 0.4789$; dose, $F_{(1,89)} = 10.07$, $p = 0.0021$; genotype \times dose, $F_{(1,89)} = 0.08954$, $p = 0.7655$]. It is worth noting that novelty-induced locomotor hyperactivity is only a poor predictor of acute cocaine responses, and observations reported here further provide evidences in favor of it (Ragu Varman et al., 2021).

Cocaine-induced behavioral sensitization is impaired in *Tmod2* KO

Repeated administration of psychostimulants such as cocaine evokes behavioral sensitization—a progressive and persistent amplification of locomotor response to the same dose of the drug. Sensitization is a hallmark of many drugs of abuse and is due to neuroadaptations in the reward circuit (Vanderschuren and Kalivas, 2000; Robinson and Berridge, 2003). Although it is only partially predictive of self-administration, a sensitization paradigm is often used to gauge plasticity in the mesolimbic circuit (Phillips, 1997). Our sensitization protocol consists of once-daily injections of saline for 4 consecutive days (test Day 1–4), followed by six, noncontingent, cocaine injections (15 mg/kg, test Day 5–10) and a saline injection on test Day 11 (Fig. 3E1). Since sensitization has been shown to be long-lasting (Steketee and Kalivas, 2011), we carry out a cocaine challenge on test Day 17 and 24, a period of 1 or 2 weeks later. Repeated administration of cocaine resulted in progressive amplification of locomotor responses in WT mice (Fig. 3E1). Intriguingly, *Tmod2* KO had a significant

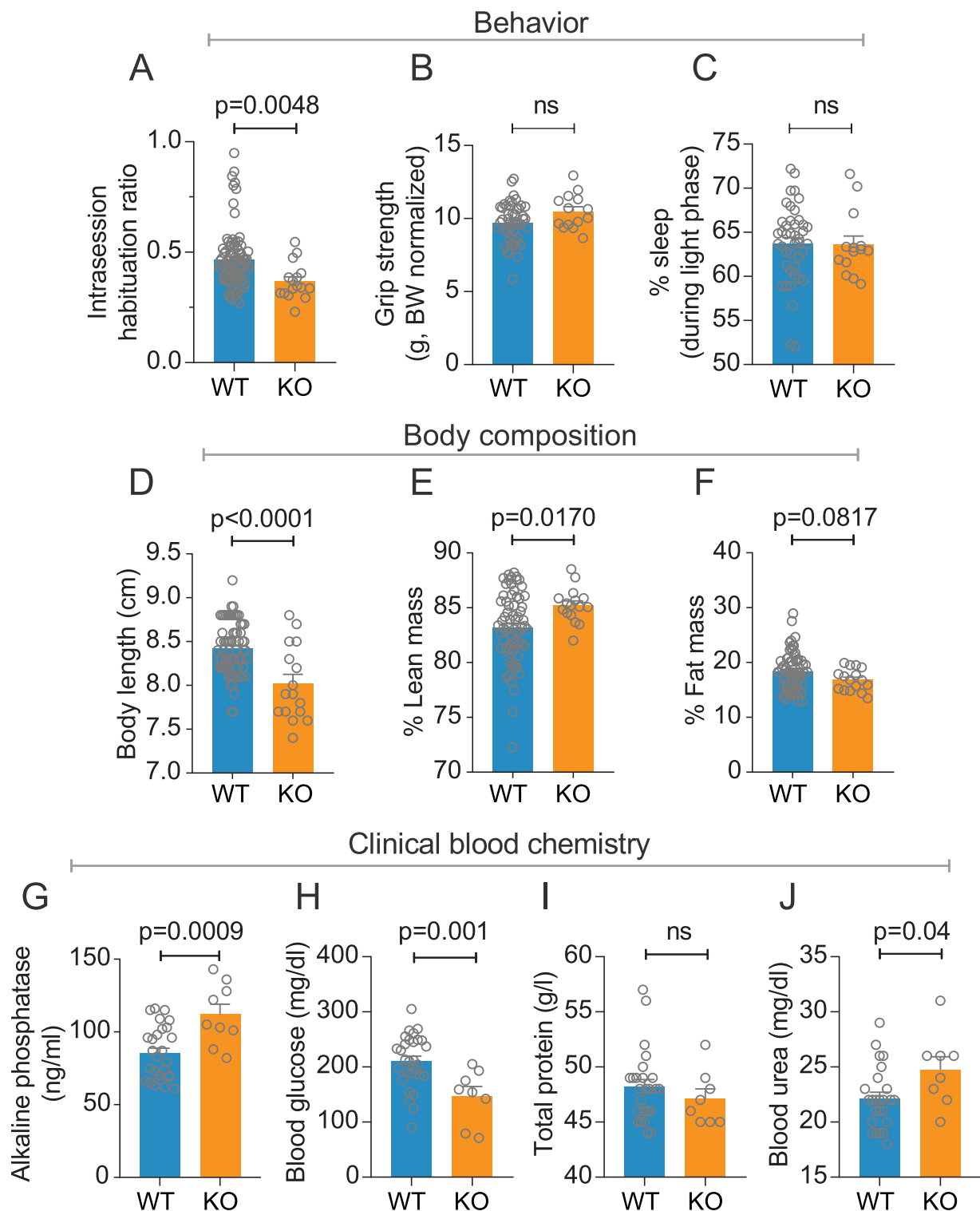


Figure 2. Other behaviors, body composition, and clinical blood chemistry parameters collected from KOMP phenotyping pipeline. **A**, intrasection habituation in open field; **B** grip strength normalized to BW; **C** % of time spent in sleep state. **D–F**, Body composition results; **D** body length in centimeters (cm); **E** percentage of lean mass; **F** percentage of fat mass. **G–J**, Clinical blood chemistry results; **G** alkaline phosphatase level; **H** blood glucose level; **I** total protein in blood; **J** blood urea level. p -values reported in the figure are obtained by unpaired t test. NS, not significant. Error bar represents SEM. All raw data retrieved from KOMP pipeline is provided as table in Extended Data Figure 1–2.

attenuation of the cocaine-induced sensitization response compared with WT [Fig. 3E1; genotype, $F_{(1,806)}=252$, $p<0.0001$; drug, $F_{(12,806)}=51.42$, $p<0.0001$; genotype \times drug, $F_{(12,806)}=11.34$, $p<0.0001$]. *Tmod2* KO mice show slight sensitized responses to the first three cocaine injections (Day 5–7) with an increase in locomotor activity, but from the fourth day onwards (Day

8–10) and on cocaine challenge days (Day 14 and 24), no further escalation in locomotor activity was observed (Fig. 3E1). It is worth noting that a weak, drug-induced sensitization response is exhibited by *Tmod2* KO mice on Day 5–7 with an early-achieved ceiling effect that stabilizes locomotor response from the eighth day onwards and persists for the rest of the protocol. Post hoc analysis

confirmed the absence of any locomotor differences between mutant and WT to acute cocaine administration (Fig. 3E1; Day 5, first cocaine administration, $p = 0.8109$). We visually inspected the recorded videos for stereotyped behaviors, another form of behavioral sensitization (Tolliver and Carney, 1994; Areal et al., 2019), but did not observe any cocaine-induced short- or long-term effects in *Tmod2* KO mice. These data indicate an impaired behavioral sensitization response in *Tmod2* KO suggestive of compromised drug-induced neuroadaptations.

Multiple exposures to a similar environmental context attenuate novelty-induced locomotor activity and lead to habituation: a form of nonassociative learning (Bolivar, 2009). In our analysis of sensitization data, we observed that *Tmod2* KO mice were not hyperactive in the open field for the entire 20 min, indicating high rates of intrasession habituation in a novel environment, which is comparable to WT (Fig. 3E1; $p > 0.01$). Similarly, intersession habituation was also comparable between *Tmod2* KO and WT controls, indicating that *Tmod2* KO does not interfere with habituation learning of the environmental context (Fig. 3E1; $p > 0.05$). Preinjection baseline periods (from -60 to 0 min) of the first 4 saline days of behavioral sensitization paradigm were used to reconfirm the open-field phenotype observed in the KOMP analysis. *Tmod2* KO exhibited persistent, elevated locomotor activity, compared with WT on Day 1 [Fig. 3E2-Day 1; genotype, $F_{(1,1100)} = 147.5$, $p < 0.0001$; time-bins, $F_{(10,1100)} = 25.1$, $p < 0.0001$; genotype \times time-bins, $F_{(10,1100)} = 0.5143$, $p = 0.8809$]. A main effect of genotype was also detected on Day 2 [Fig. 3E2-Day 2; genotype, $F_{(1,1100)} = 4.995$, $p = 0.0256$; time-bins, $F_{(10,1100)} = 6.166$, $p < 0.0001$; genotype \times time-bins, $F_{(10,1100)} = 1.007$, $p = 0.4356$]; however, the post hoc analysis revealed that the time-bins significance was restricted to the first, 5 min bin with WT having more locomotor activity compared with *Tmod2* KO (Fig. 3E2-Day 2; Sidak's multiple comparison, $p = 0.0245$). On Day 3 [Fig. 3E2-Day 3; genotype, $F_{(1,1100)} = 2.298$, $p = 0.1298$; time-bins, $F_{(10,1100)} = 18.07$, $p < 0.0001$; genotype \times time-bins, $F_{(10,1100)} = 0.9725$, $p = 0.4656$] and Day 4 [Fig. 3E2-Day 4; genotype, $F_{(1,1100)} = 0.5777$, $p = 0.4474$; time-bins, $F_{(10,1100)} = 14.34$, $p < 0.0001$; genotype \times time-bins, $F_{(10,1100)} = 1.211$, $p = 0.2794$], a main effect of genotype and post hoc time-bins comparison failed to detect any statistically significant difference between *Tmod2* KO and WT. Similarly, on Day 1, center distance traveled (Fig. 3E3,D1; $t = 5.386$; $p < 0.001$) and time spent in the center (Fig. 3E4,D1; $t = 6.559$; $p < 0.001$) are significantly higher in *Tmod2* KO recapitulating the results obtained from KOMP data. However, from the second day onwards (D2–D4; Fig. 3E3–4), these anxiety parameters are comparable in both the genotypes, indicating an amplified habituation response to a less novel, familiar environmental context in *Tmod2* KO. This analysis demonstrates that the hyperactivity in *Tmod2* KO is a specific response toward environmental novelty that is only seen on the first day of the open-field test and is not due to general hyperactivity. Thus, habituation, which is a form of nonassociative learning, is preserved and perhaps increased in *Tmod2* KO. Combined, these data suggest that experience and pathway-specific neuroadaptations that mediate habituation are functional in *Tmod2* KO, while specific deficits are seen in neuroadaptations that mediate behavioral sensitization.

Failure to acquire cocaine self-administration

Although locomotor sensitization is an established model of drug-induced plasticity and neuroadaptations, it is only partially predictive of voluntary drug intake (Phillips, 1997). Goal-directed behavior and motivation to procure drug is conventionally tested by IVSA, the gold standard technique in the addiction

field (Mello and Negus, 1996; Sanchis-Segura and Spanagel, 2006; Thomsen and Caine, 2007; Belin-Rauscent et al., 2016). Therefore, we assessed cocaine acquisition and dose–response in *Tmod2* KO and WT using the IVSA paradigm.

To assess cocaine IVSA performance, we performed repeated measures or one-way ANOVA using the number of lever presses or the number of infusions as dependent measures. Genotype (*Tmod2* KO, WT) and sex were between-subject factors. Session (Day 1–5) was a within-subject factor. When lever presses were used as the dependent measure, lever (active, inactive) was used as a second within-subject factor. WT mice rapidly learned to lever press for cocaine (Fig. 3F) as indicated by a significant increase in active lever presses across sessions (Day 1 vs Day 5, $p = 0.05$) and a significant dissociation between the active and inactive levers (active vs inactive on Session 5, $p = 0.002$). In contrast, *Tmod2* KO mice failed to acquire cocaine infusions as indicated by a failure to significantly increase active lever presses across sessions (Day 1 vs Day 5, $p = 0.67$) and a failure to dissociate between the active and inactive levers (active vs inactive on Day 5, $p = 0.82$). This lever pressing pattern resulted in WT mice infusing significantly more cocaine across the first five sessions relative to *Tmod2* KO mice (Fig. 3F, inset; $p < 0.05$). Lever pressing was mediated by strain and lever as indicated by significant main effects of strain [$F_{(1,26)} = 5.00$; $p = 0.03$] and lever [$F_{(1,26)} = 12.84$; $p = 0.001$], as well as a significant strain \times lever interaction [$F_{(1,26)} = 4.64$; $p = 0.04$]. Interestingly, active lever press was comparable on Day 1 indicating that general exploration and responses to operant cues are able to evoke behavior directed to the levers in *Tmod2* KO. However, either neutral or aversive outcome of active lever press rapidly extinguishes the future responses toward the active lever.

Comparison of WT and *Tmod2* KO mice for cocaine IVSA was limited to the acquisition phase because WT mice stabilized at the 1.0 mg/kg/infusion acquisition dose and advanced to the dose–response curve stage by session five. *Tmod2* KO mice were tested for a total of 24 sessions (Fig. 3F) to test if they could learn to acquire cocaine if sufficient exposure was provided. During these 24 sessions, *Tmod2* KO mice failed to significantly increase response on the active lever and failed to dissociate between the active and inactive levers as indicated by nonsignificant main effects of lever ($p = 0.95$) and session ($p = 0.24$) as well as a nonsignificant lever \times session interaction ($p = 0.33$). Since the mice failed to acquire, cocaine IVSA testing was terminated for *Tmod2* KO mice after Session 24. IVSA results demonstrate that the dose that is reinforcing to WT mice is not reinforcing to KO mice and indicates either general reward deficits, learning deficits in an operant task, or both. Additionally, modified cocaine metabolism could also contribute to the lack of acquisition and low locomotor sensitization in *Tmod2* KO.

Intact motivation toward natural reward

In order to investigate the responsiveness to natural reward and to rule out a general deficit in reward-based learning, we subjected mice to a two-bottle sucrose preference test. Both strains show comparable motivation and preference toward 4% sucrose solution provided in the sucrose preference test (Fig. 3G; $t = 1.055$; $p = 0.3108$). Therefore, inability of *Tmod2* KO to self-administer cocaine is not because of a general deficit in reward sensing and responding neural circuitry.

Cocaine metabolism is unaffected in *Tmod2* KO mice

In vivo cocaine metabolism is an important determinant of its pharmacokinetics and tissue bioavailability that could modulate

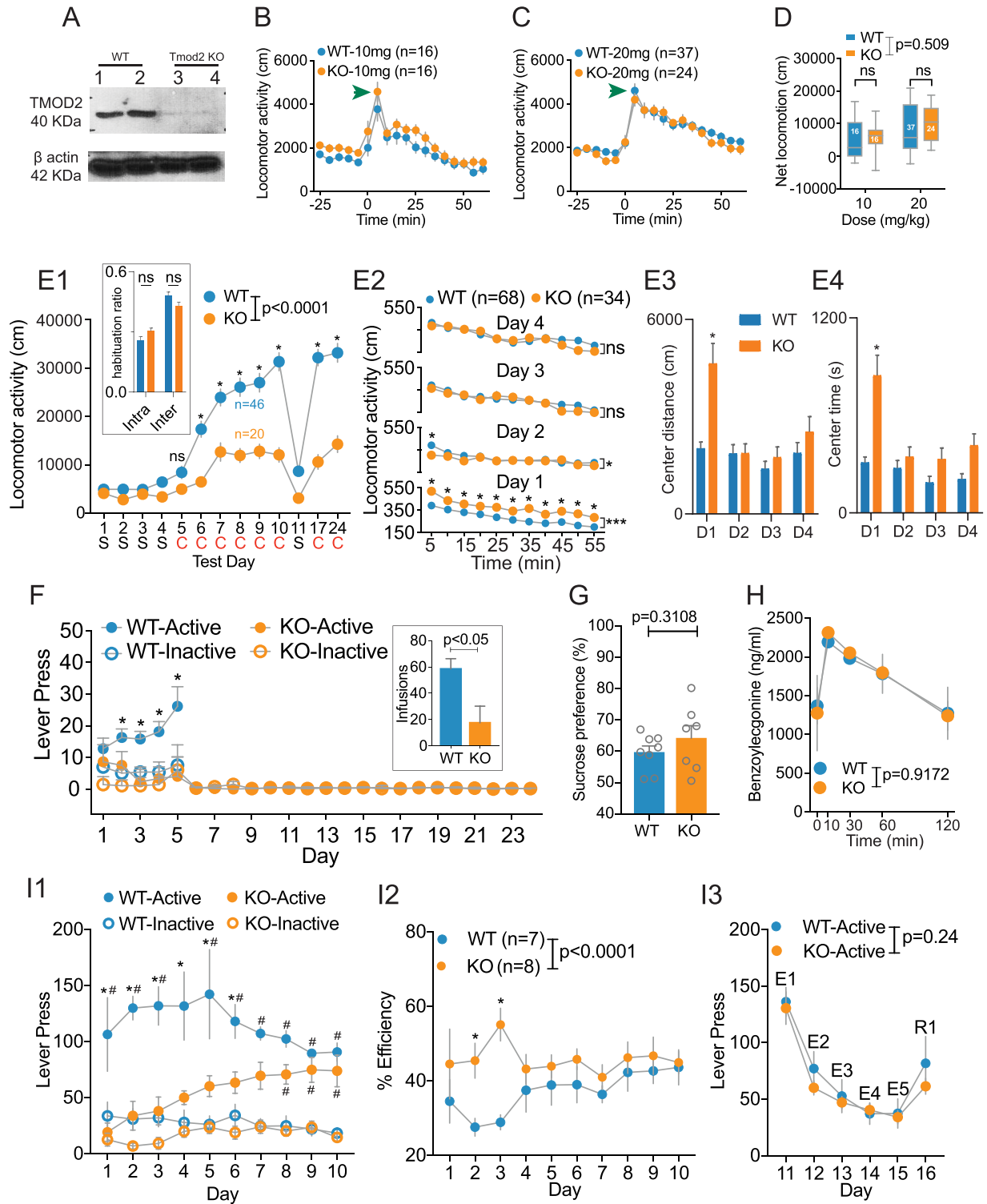


Figure 3. Comprehensive addiction phenotyping in *Tmod2* KO reveals deficits in cocaine sensitization and IVSA. **A**, Qualitative assessment of the absence of TMOD2 protein in cortical lysate from KO brain. **B**, Locomotor response following acute injections of low (10 mg/kg i.p.) and **C** high (20 mg/kg i.p.) doses of cocaine. Green arrowhead indicates locomotor artifact due to injection procedure. **D**, Net locomotor activity following low and high dose of cocaine. **E1–E4**, Results obtained from locomotor sensitization protocol. **E1**, Graph's x-axis show day and corresponding treatment (S, saline; C, cocaine) on that day. Figure inset shows intra- and inter-session habituation learning in open-field arena. **E2**, Day 1–4 baseline locomotor activity. **E3**, Mean center distance traveled and **E4** time spent in the center during the baseline period of Day1–4. **F**, Active and inactive lever presses on Day 1–24 of cocaine IVSA testing. Inset shows the number of cocaine infusions. **G**, Sucrose preference. **H**, Cocaine metabolite benzoylcocaine concentration in plasma at different time points following cocaine (20 mg/kg) injections. **I1–I3**, Operant conditioning using palatable food as a reinforcement resulted in **(I1)** active and inactive lever presses; **(I2)** total sucrose pellets obtained by the total number of active and inactive lever presses is calculated as percent efficiency; **(I3)** extinction sessions (**E1–E5** on Day 11–15) and reinstatement (R1 on day 16) of reward behavior. Error bar represents SEM. NS, not significant. *Bonferroni's multiple comparison post hoc test detected significant differences ($p < 0.01$) between WT and KO mice. ***main effect of genotype detected using the two-way ANOVA [(F10, 1100) = 25.10; $p < 0.0001$]. #Significant difference between inactive and active lever presses within the same genotype ($p < 0.01$).

a drug-induced addiction-like phenotype. To test cocaine metabolism in these mice, we carried out a biochemical analysis for the primary cocaine metabolite benzoylecgonine (Benuck et al., 1987) by injecting mice with cocaine (20 mg/kg) and collecting blood from the submandibular vein at 0, 10, 30, 60, and 120 min following injections. No significant differences in the level of the cocaine metabolite benzoylecgonine was observed between *Tmod2* KO and WT mice for any of the sampled time points, indicating that cocaine metabolism is not affected in these mutants (Fig. 3H).

Delayed learning ability in operant assay

Since *Tmod2* has previously been shown to regulate learning and memory deficits in mice (Cox et al., 2003) and has been linked to intellectual deficits in human GWAS studies (Davies et al., 2018; Hill et al., 2019), we tested whether the KO mice were capable of learning an operant task. Operant conditioning relies on associative learning, and therefore the impairment to acquire cocaine in the IVSA paradigm could be due to learning deficits. We investigated operant learning in *Tmod2* KO mice for palatable food reward as a reinforcement stimulus. *Tmod2* KO mice took significantly a greater number of trials to learn the association between active lever and palatable food reward and to discriminate between the active and inactive levers (Fig. 3I1). In contrast, WT mice learned to discriminate between the active and inactive levers by the end of Day 1 and demonstrated stronger associative learning than *Tmod2* KOs [Fig. 3I1; genotype and lever, $F_{(3,242)} = 117.9$, $p < 0.0001$; day, $F_{(9,242)} = 0.7612$, $p = 0.6525$; genotype and lever \times day, $F_{(27,242)} = 1.347$, $p = 0.1244$]. In *Tmod2* KO, statistically significant discrimination between the active and inactive levers emerges on Day 8, and from Day 7 onwards, active lever presses by KO and WT are comparable (Fig. 3I1). Surprisingly, the operant efficiency (the number of sucrose pellets obtained divided by the total number of active and inactive lever presses) was slightly better in *Tmod2* KO. We hypothesize that this is due to compulsive lever pressing by WT mice during initial trials (Fig. 3I1; Day 1–5) which ignores the 20 s time-out period between two successful (paired with reward) active lever presses [Fig. 3I2; genotype, $F_{(1,115)} = 19.37$, $p < 0.0001$; day, $F_{(9,115)} = 0.7663$, $p = 0.6477$; genotype \times day, $F_{(9,115)} = 1.554$, $p = 0.1375$]. On extinction sessions (Fig. 3I3, E1–E5 on Day 11–15) during which neither reward nor operant cue (cue light off) was presented, both *Tmod2* KO and WT exhibited a comparable, rapid decline in the number of lever presses that was previously paired with reward indicating that extinction-induced associative learning is intact in both the genotypes [Fig. 3I3; genotype $F_{(1,66)} = 1.405$, $p = 0.2401$; day, $F_{(5,66)} = 18.72$, $p < 0.0001$; genotype \times day, $F_{(5,66)} = 0.2839$, $p = 0.9203$]. Rebound of behavior directed toward the active lever with one single reinstatement session was also comparable between *Tmod2* KO and WT mice (Fig. 3I3; R1, Day 16, Sidak's post hoc test, $p = 0.79$). Thus, as shown previously, *Tmod2* KO mice have a deficit in learning (Cox et al., 2003). However, given enough time and trials, *Tmod2* KO mice learn operant tasks. In trials with food reward, *Tmod2* KO mice were indistinguishable from WT mice from Day 7, whereas with cocaine as a reinforcement, *Tmod2* KO failed to learn even after 24 d trial, which leads us to conclude that there is a deficit in cocaine-induced reward learning in *Tmod2* KO mice.

Reduced brain volume and absence of differentially coexpressed transcripts

Since neuron-specific TMOD2 regulates actin stabilization and plays an important role in dendritic arborization, and synapse formation (Gray et al., 2016; Omotade et al., 2018), we investigated if

regional and gross morphological changes are seen in *Tmod2* KO brains. We carried out MRI analysis, a well-established diagnostic and translational tool in clinical and preclinical research, and discovered that the whole-brain volume is significantly decreased in *Tmod2* KO relative to the WT mice (Fig. 4A,B; -8.8% ; $p = 1.5 \times 10^{-9}$). The extent of volume loss appears to be greater in the white matter, as the overall changes for the gray and white matter were -8.2% ($p = 4 \times 10^{-9}$) and -14.7% ($p = 7 \times 10^{-12}$), respectively (Fig. 4A). The volumes of 182 structures (using combined left–right volumes) were computed for all animals. While the 20–25% decrease in BW in 10–11-week-old *Tmod2* KO (Fig. 1F) may explain some of this change, proportional weight change is not generally a predictor of proportional brain volume change in adult rodents (Agrawal et al., 1968; Bailey et al., 2004).

For the absolute volume analysis, a total of 109 structures were observed to be significantly different for the *Tmod2* KO mice ($q < 0.05$), all but one of which were volume decreases. Prominent changes included regions of the cerebellum, much of the cortex, the corpus callosum, the thalamus, the hippocampus, and, with relevance to the mesolimbic system, the striatum and midbrain (summarized in Fig. 4-1). However, given the overall difference in brain size, we also normalized results by expressing structure volume as a percentage of whole-brain volume, and then comparing results. A total of 39 brain structures showed a significant difference in relative volume (Fig. 4B,C). Several of the regions that decreased in absolute size were still observed to be decreased in this analysis, especially the white matter regions (Fig. 4B,C, blue bars), but several structures also appeared relatively larger (Fig. 4B,C, red bars), including the hypothalamus, olfactory bulbs, nucleus accumbens, and basal forebrain.

Next, we attempted to detect any molecular differences that may have resulted from the deletion of *Tmod2* gene. Specifically, we hypothesized differences in cell-type constituency, cell loss, neuroinflammation, neurodegeneration, or general developmental deficits that may be cell-type specific and thus would lead to changes in gene coexpression networks that could be detected by monitoring genome-wide gene expression (Parikhshak et al., 2015; Srinivasan et al., 2016). We carried out RNAseq analysis from the striatum and cortex of naive adult mice (3 M/3 F) for *Tmod2* KO and WT animals. A poly(A)-enriched RNA-sequencing library was generated at a depth of 40–50 million reads. Data were analyzed using BioJupies (Torre et al., 2018). As expected, we detected a clear difference in *Tmod2* RNA levels in both tissues (Fig. 4D; FDR < 0.05 ; $q = 0.005$ and 0.002 in the cortex and striatum, respectively). Unexpectedly, we observed very few other genes that were significantly misregulated (Fig. 4-2). As a control analysis, we compared the striatum and cortex gene expression in WT animals and found over 7,439 genes (Fig. 4-2) that were differentially expressed in these regions (Fig. 4E; FDR < 0.05). These genomic results indicate that there are no changes in gene coexpression networks that are detectable using bulk RNAseq analysis given our power. Thus, even though *Tmod2* KOs have emotionality phenotypes associated with changes in brain volume, the transcriptomic analysis indicates a neural system that, for the most part, has a normal constituency. This led us to hypothesize that the observed behavioral changes are due to functional differences that may be detectable using electrophysiological methods.

Enhanced cortical excitability during development and adulthood

Since TMOD2 regulates dendritic arborization (Gray et al., 2017; Omotade et al., 2018), synapse density and maturation, and

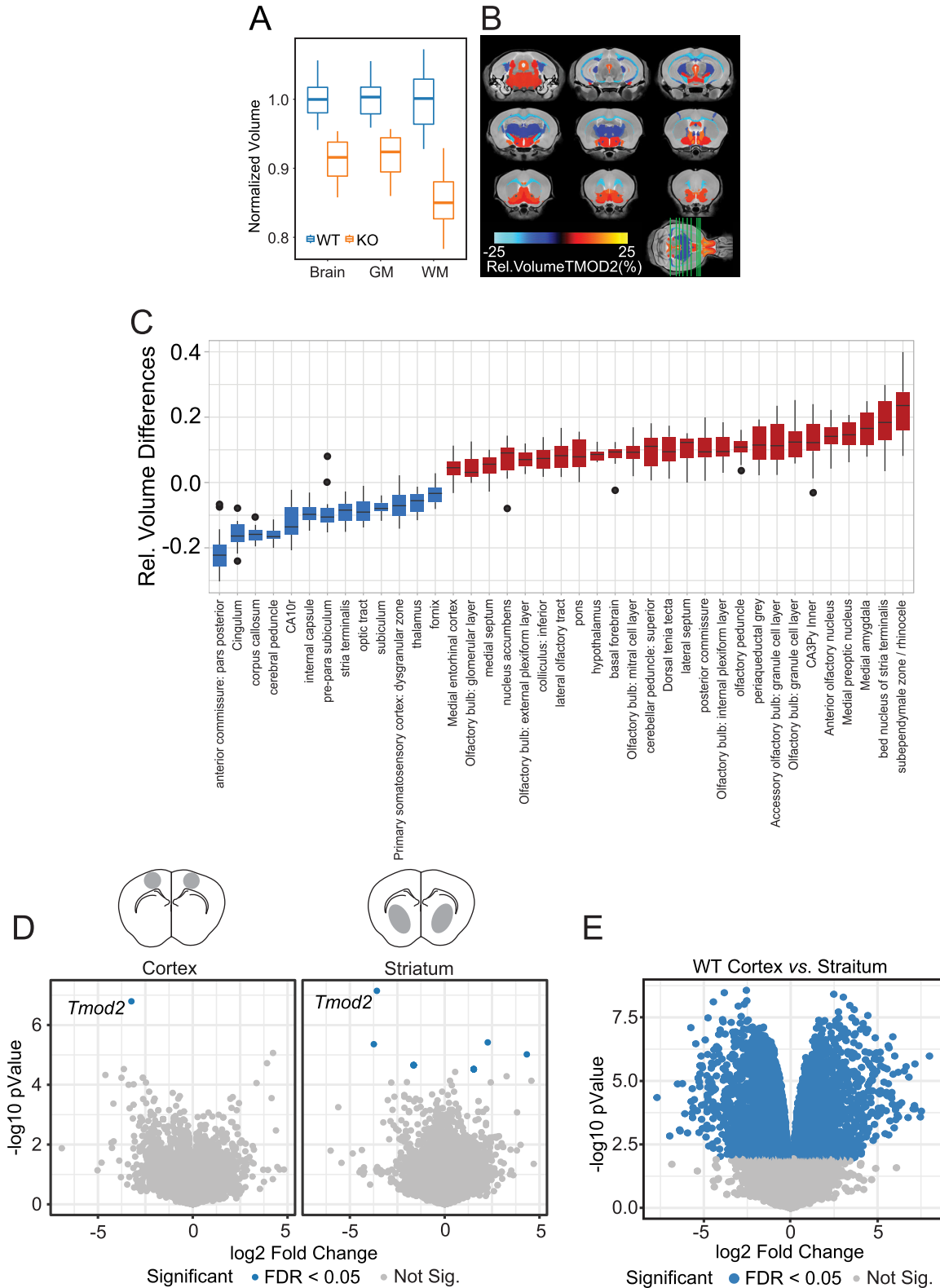


Figure 4. MRI and bulk RNAseq analysis on WT and KO brains. **A**, Normalized brain volume comparison. **B**, KO strain differences based on relative volumes. Color overlays indicate volume changes referenced to the WT. **C**, Relative volume differences of KO brain regions. Blue and red boxes indicate relative decrease and increase in volume of the labeled brain region. Most of the blue boxes are associated with white matter regions in the brain. **D**, Schematic of cortical punches obtained from the M1 subregion and dorsoventral striatum (gray-highlighted region) along with volcano plots of cortical and striatal differentially expressed genes in KO relative to WT. **E**, Analysis of differentially expressed transcript in the cortex and striatum found numerous hits indicating strong region-specific transcription profile. Error bar represents SEM. Blue circle indicates a transcript that fulfills threshold criteria. Summary of absolute brain volume of different brain regions using MRI is provided as table in Extended Data Figure 3-1. RNAseq analysis data from the striatum and cortex of naive adult mice for *Tmod2* KO and WT animals are provided as table in Extended Data Figure 3-2.

synaptic plasticity (Cox and Zoghbi, 2000; Gray et al., 2016; Omotade et al., 2018), we hypothesized that the firing properties of neurons might be modified due to the altered synaptic connectivity. To test this, we harvested cortical cells from P0–P1 pups and quantified the spontaneous firing features of cultured neurons on MEA plates. We also tested the effect of GABA-A receptor and AMPA receptor antagonism on spontaneous activity (Fig. 5B). MEA captures in vitro real-time electrophysiological activity and interconnectivity between cultured neurons permitting recreation of complex firing patterns and detection of deficits in a high-throughput fashion. *Tmod2* protein expression was detected in the rat brain as early as embryonic Day 14 (E14) and attained adult-level expression by E19 (29). Embryo imaging data collected on *Tmod2* KO by KOMP phenotyping reveals robust, nervous system-specific LacZ expression driven by the *Tmod2* promoter at E12.5 (Fig. 5A). This early developmental expression of *Tmod2* in mouse embryos suggests a critical function that could be compromised in *Tmod2* KO. *Tmod2* KO cortical neurons discharged at a higher frequency under a drug-free condition (Fig. 5C, E1; $t = 3.547$; $p = 0.0045$). PTX, a potent GABA-A receptor blocker, failed to affect the firing rate in *Tmod2* KO cultures, whereas WT neurons respond with a threefold change in the firing rate (Fig. 5E2; $t = 2.899$; $p = 0.0327$). This could be due to fewer functional, membrane-bound GABA-A receptors in *Tmod2* KO neurons or the absence of presynaptic GABAergic innervations or both. Absence or decrease in inhibitory tone to cultured neurons could also explain the increased firing rate in *Tmod2* KO cortical cultures. Similarly, *Tmod2* KO neurons produce significantly more bursts under the drug-free baseline condition (Fig. 5F1; $t = 4.392$; $p = 0.0011$). PTX application resulted in an eightfold increase in burst number in WT neurons and has no effect on *Tmod2* KO neurons suggesting altered GABA receptor availability or GABAergic synapses or both (Fig. 5F2; $t = 4.538$; $p = 0.0094$). NBQX application prevented bursting in WT cortical neurons, while the *Tmod2* KO neurons showed a similar tendency, but did not reach our statistical cutoff (Fig. 5F2; $t = 2.391$; $p = 0.0863$). Synchronicity among cultured neurons to fire simultaneously is significantly elevated in *Tmod2* KO neurons (Fig. 5G1; $t = 5.133$; $p = 0.0003$). PTX application resulted in a fourfold increase in firing synchronization of WT cortical neurons and had no effect on *Tmod2* KO neurons (Fig. 5G2; $t = 4.947$; $p = 0.003$). As anticipated, NBQX application mitigates the synchrony index in WT neurons but not in *Tmod2* KO (Fig. 5G2; $t = 3.16$; $p = 0.0134$). These results clearly demonstrate that *Tmod2* KO neurons in culture exhibit enhanced cortical excitability along with modified excitation/inhibition ratio during early developmental stages.

To test whether neuronal excitability seen in early postnatal neurons persists in adult *Tmod2* KO, we compared intrinsic properties of prelimbic cortical (Fig. 5H1–7) and accumbens shell neurons (Fig. 5I1–5) in KO and WT using whole-cell recording in acute brain slices. Naive mice were killed and brain slices containing prelimbic and accumbens region neurons were recorded. *Tmod2* KO cortical neurons fired more action potential spikes in response to depolarizing current steps than WT neurons (Fig. 5H1–2). *Tmod2* KO neurons showed slightly higher resting membrane potentials than WT neurons (Fig. 5H3), but no change in input resistance or whole-cell capacitance (Fig. 5H4–5). The action potential threshold (39.51 ± 0.46 mV in WT and -38.6 ± 0.53 in *Tmod2* KO; Fig. 5H6) and afterhyperpolarization (AHP) amplitude (12.11 ± 0.62 mV in WT and 13.48 ± 0.76 mV in *Tmod2* KO; Fig. 5H7) are statistically comparable between genotypes indicating functional similarity of voltage-gated sodium channels and potassium channels. *Tmod2* KO accumbens shell neurons are also more excitable

than WT (Fig. 5I1, 2), but no change in resting membrane potential was observed (Fig. 5I3). The input resistance is slightly higher in *Tmod2* KO neurons (Fig. 5I4), and whole-cell capacitance is comparable between both genotypes (Fig. 5I5). The action potential threshold (-35.69 ± 0.98 mV in WT, -35.67 ± 0.59 mV in *Tmod2* KO; Fig. 5I6) and AHP amplitude (12.05 ± 1.03 mV in WT and 12.07 ± 0.52 mV in *Tmod2* KO; Fig. 5I7) are statistically comparable between genotypes. Therefore, *Tmod2* deletion results in an increase in excitability of prelimbic pyramidal neurons, and medium spiny neurons of the accumbens shell, indicative of its role in determining the firing features of neurons and their interconnectivity.

Distinct naive and cocaine-induced synaptic properties

Action potential-independent, spontaneous release of neurotransmitters from presynaptic neurons and measurement of the miniature excitatory or inhibitory postsynaptic currents is a standard method to assess the baseline and drug-induced alteration in synaptic coupling between neurons. Noncontingent cocaine administration induces widespread modifications of synaptic properties in reward-related brain regions, triggering maladaptive reward learning (Grueter et al., 2012). These synaptic alterations have been extensively characterized in the nucleus accumbens and establish both effect and causality of cocaine abuse (Kauer and Malenka, 2007). *Tmod2* KO mice have an attenuated locomotor sensitization response to repeated cocaine administration and perform poorly in an IVSA paradigm. We hypothesized that drug-induced synaptic changes are either missing or weak in *Tmod2* KO resulting in a drug-resistant phenotype. Mice were treated with a once-daily injection of either saline or cocaine for 5 consecutive days, killed following 2–5 d of abstinence, and brain slices containing accumbens region neurons were recorded (Fig. 6B). We compared mEPSC (Fig. 6C1) and mIPSC (Fig. 6D1) in medium spiny projection neurons of the accumbens shell (Fig. 6A) in drug-naive (saline-injected) and drug-experienced (cocaine-injected) mice using ex vivo whole-cell recording in brain slices. The mean amplitude of mEPSCs is significantly elevated in naive *Tmod2* KO compared with naive WT neurons (Fig. 6C2), which suggests an increased number or function of AMPA receptors on patched accumbens neurons (Malenka and Nicoll, 1999). Cocaine treatment increases mEPSC frequency in WT but not *Tmod2* KO neurons (Fig. 6B3) and suggests that repeated cocaine exposure fails to induce synaptic changes typically associated with chronic cocaine exposure (Robinson and Kolb, 2004). No significant effect of treatment or genotype was observed in either mEPSC rise or decay time which indicates a lack of alterations in the postsynaptic properties of AMPA receptors (Fig. 5C4, 5).

Medium spiny neurons of the accumbens shell receive inhibitory afferents from local interneurons, cortex and VTA (Ishikawa et al., 2013; Li et al., 2018). There is no change in the mIPSC amplitude in WT and KO with or without drug exposure (Fig. 6D2). However, the mIPSC frequency is higher in naive KO neurons than naive WT neurons, and cocaine exposure increases the mIPSC frequency in KO but not WT neurons (Fig. 6D3). The elevated mIPSC frequency in *Tmod2* KO could be a neurophysiological homeostatic adaptation to compensate for increased excitability of accumbens shell neurons due to modified intrinsic and excitatory synaptic properties (Kilman et al., 2002). The rise and decay time of mIPSCs are not different in WT and KO and unaffected by cocaine exposure (Fig. 6D4, 5). Combined, investigation of synaptic properties indicates preexisting and drug-induced differences in excitatory pre- and postsynaptic neurotransmission,

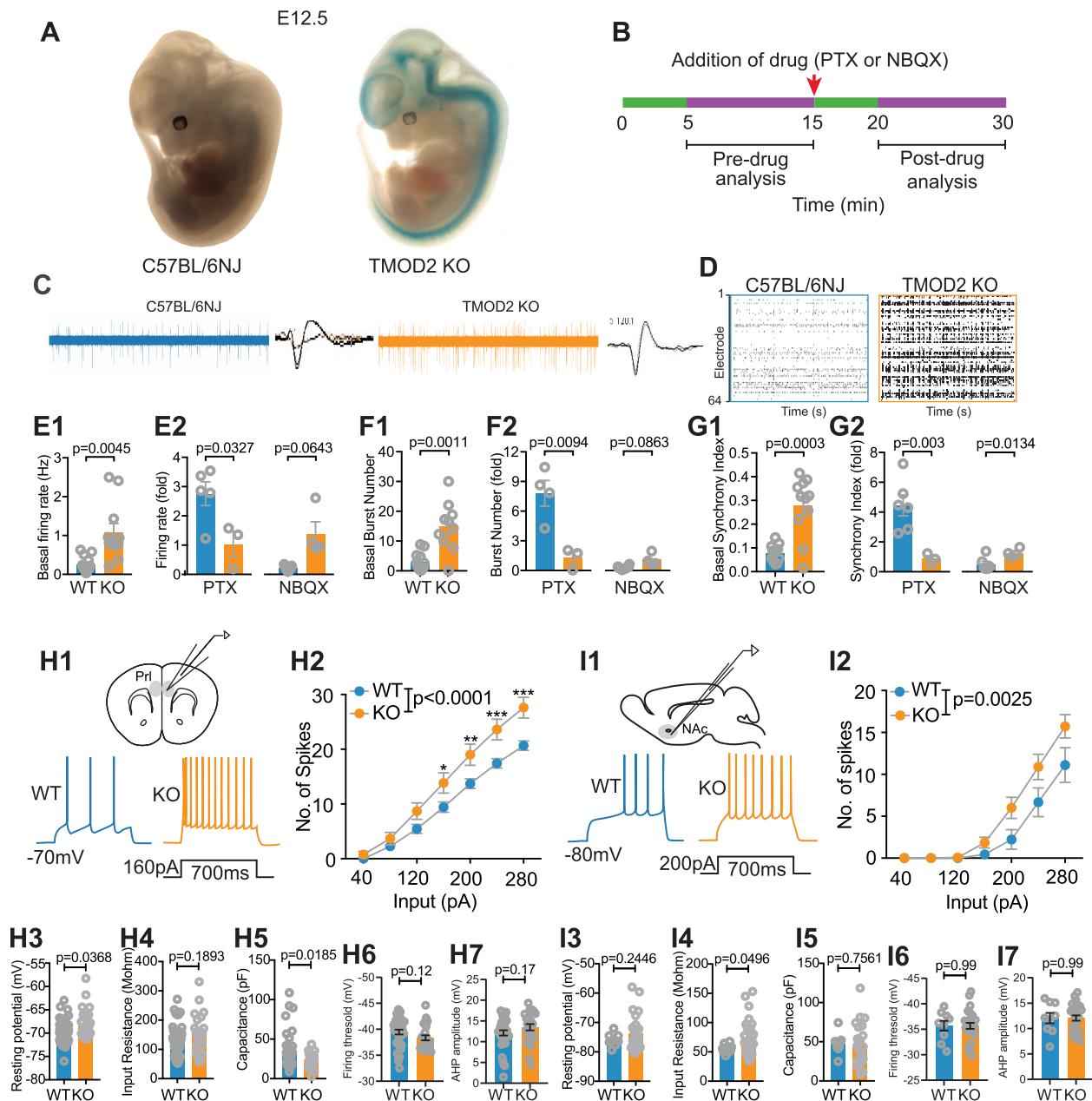


Figure 5. Characterization of spontaneous firing features of early postnatal cortical neurons and intrinsic properties of reward regions in the adult brain. **A**, LacZ expression in KO embryo (E12.5) driven by *Tmod2* promoter and the absence of expression in WT. **B**, Timeline of multielectrode array (MEA) recordings of cultured cortical neurons. **C**, Raw traces of spiking activity and off-line spike sorting captured by MEA electrodes. **D**, Representative raster plots of spontaneous spiking activity in WT and KO neurons across 64 electrodes. **E1**, Baseline spiking activity obtained from predrug window. **E2**, Spiking activity following PTX and NBQX application in bath. **F1**, Number of burst detected in 10 min predrug period and **F2**, following PTX and NBQX application. **G1**, Synchrony index; (**G2**) synchrony index following PTX and NBQX application. **H1–H5**, Intrinsic properties of adult, prelimbic pyramidal neurons. $N = 23–38$ neurons per genotype; 3–4 mice per genotype. **H1**, Schematic of whole-cell recordings performed in the fifth layer of the prelimbic cortex along with representative action potentials recorded by applying 160 pA for 700 ms. **H2**, Mean number of spikes for a given (x -axis) magnitude of injected current. **H4**, Input resistance. **H5**, Whole-cell capacitance. **H6**, firing threshold in millivolts (mV); (**H7**) AHP amplitude. **I1–I5**, Intrinsic properties of adult, accumbens shell medium spiny neurons ($N = 9–28$ neurons per genotype; 3–4 mice per genotype). **I1**, Schematic of recorded brain region and sample traces at 200 pA. **I2**, Mean number of spikes for a given (x -axis) magnitude of injected current. **I3**, Resting membrane potential. **I4**, Input resistance. **I5**, Whole-cell capacitance. Error bar represents SEM. **I6**, firing threshold. **I7**, AHP amplitude. p -values reported in the figure are obtained by unpaired t test. Error bar represents SEM. * $p < 0.05$, ** $p < 0.01$, *** $p < 0.001$. E12.5, embryonic Day 12.5. PTX, GABA-A receptor blocker. NBQX, AMPA receptor antagonist. Prl, prelimbic. NAC, nucleus accumbens.

along with augmented presynaptic inhibitory neurotransmission. These data provide a mechanistic underpinning for the lack of sensitization and acquisition in the IVSA paradigm.

Discussion

Our work describes a critical role for *Tmod2* in drug-induced behavioral sensitization and voluntary drug intake. *Tmod2* has been

weakly linked to risky drug use in humans, and its gene expression and protein levels are dynamic upon drug exposure in animal models (Iwazaki et al., 2006; Li et al., 2008; Lesscher et al., 2012; Tapocik et al., 2013; Zhang et al., 2013; Zhu et al., 2016; Polimanti et al., 2017; Oliver et al., 2018). We provide addiction-relevant behavioral data that *Tmod2* regulates cocaine-induced locomotor sensitization and voluntary self-administration of cocaine, but not acute

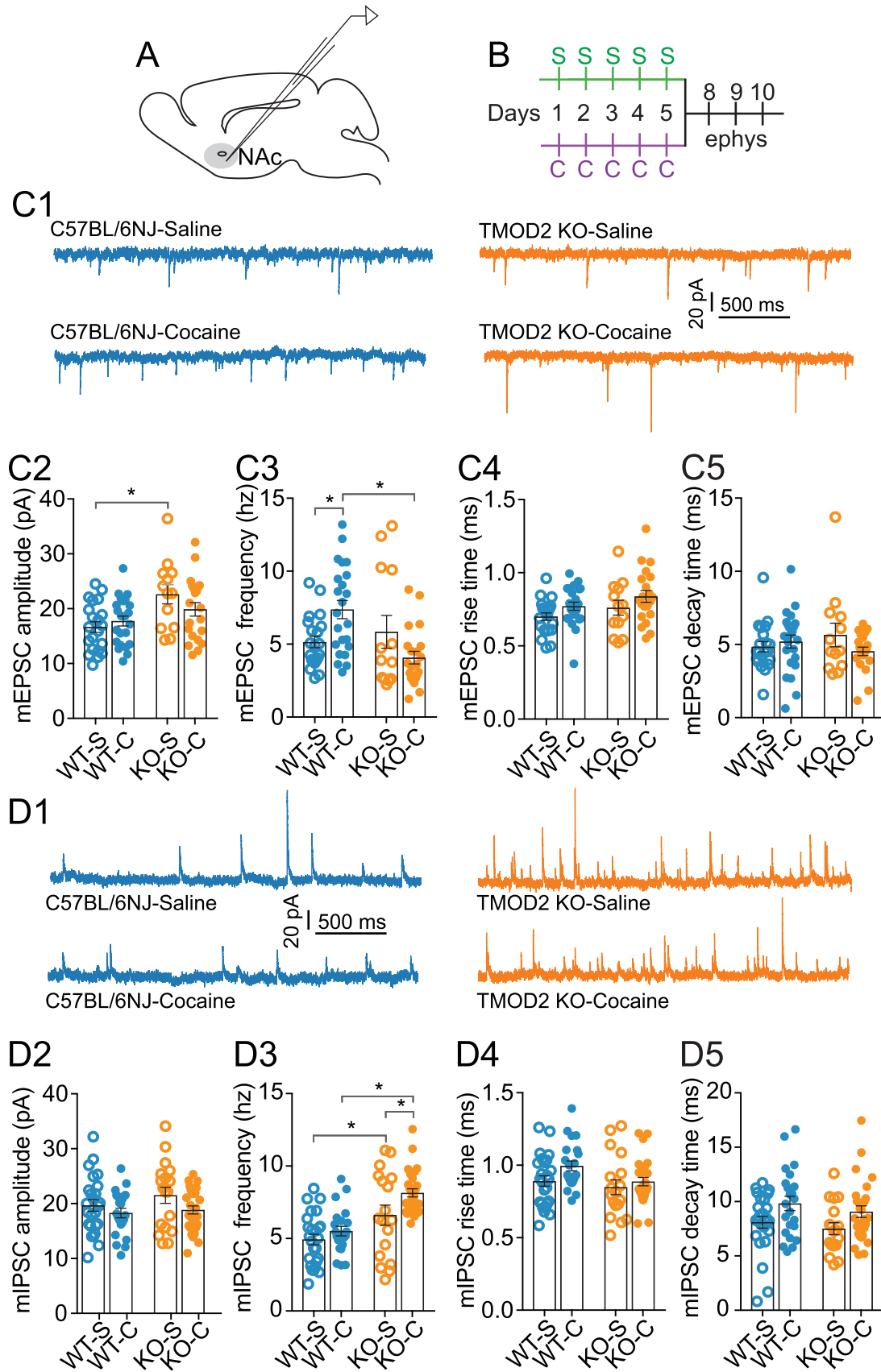


Figure 6. Electrophysiological characterization of glutamatergic and GABAergic synaptic transmission in accumbens shell medium spiny neurons. **A**, Schematic of sagittal section of mouse brain containing recorded nucleus accumbens shell subregion. **B**, Timeline of sensitization protocol in two groups. **C1**, representative traces showing mEPSCs at holding potential of -80 mV in the presence of $0.5 \mu\text{M}$ TTX in saline (top) or cocaine (bottom) injected WT and KO mice. **C2**, mEPSC amplitude; **C3** mEPSC frequency; (**C4**, **C5**) mEPSC rise and decay time. Saline group: $N = 13\text{--}16$ neurons per genotype, 3–4 animals per genotype; cocaine group: ($N = 22\text{--}27$ neurons per genotype, 4–5 animals per genotype). **D1**, representative traces showing mIPSCs at holding potential of $+5$ mV in presence of $0.5 \mu\text{M}$ TTX in saline (top) or cocaine (bottom) injected WT and KO mice. **D2**, mIPSC amplitude; **D3**, mIPSC frequency (**D4**, **D5**) mIPSC rise time and decay time. Saline group: $N = 18\text{--}27$ neurons per genotype, 3–4 animals per genotype; cocaine group: $N = 25\text{--}31$ neurons per genotype, 4–5 animals per genotype. Error bar represents SEM. * $p < 0.01$.

locomotor activation to cocaine. *Tmod2* mediates dendritic branching, spine maturation and density, and synaptic plasticity, the key components of experience-induced learning and memory including addiction (Cox et al., 2003; Hu et al., 2014; Gray et al., 2016; Omotade et al., 2018). Concordantly, we find that drug-induced plasticity is affected in these knock-outs with the deletion of *Tmod2* leading to an imbalance of excitatory and inhibitory signaling as well as compromised synaptic plasticity in the mesolimbic reward circuit. Combined, the behavioral and electrophysiological data indicate neuromodulations that mediate transition to addiction are compromised in the absence of *Tmod2*.

The structural and functional plasticities of synapses are the fundamental mechanisms that underlie addiction even though the role of actin in this process remains controversial (Russo et al., 2010; Miller et al., 2012; Rothenfluh and Cowan, 2013; Ly et al., 2018). Acute or chronic cocaine exposure, as well as abstinence, facilitates dendritic spine outgrowth and spine density in reward-related brain regions such as the prefrontal cortex and nucleus accumbens (Robinson and Kolb, 1999, 2004; Norrholm et al., 2003; Cahill et al., 2017; Dos Santos et al., 2017). Our previous study established a role of *Cyfp2*, a component of the WAVE regulatory complex that mediates branched actin formation in cocaine responses. We demonstrated that a *Cyfp2* mutation that exists in certain C57BL/6 substrains leads to altered acute and sensitized responses to cocaine (Kumar et al., 2013). The role of actin-regulating *Tmod2* in addiction-related behaviors has previously been unclear. Here we report that *Tmod2* KO mice exhibit endophenotypes that are predictive of addiction, but surprisingly exhibit resistance to drug-induced behaviors and associated neuroadaptations. Typically, hyperactivity, novelty reactivity, anxiety, and risk-taking behaviors are associated with increased risk of addiction liability in humans and animal models (Dellu et al., 1996; Davis et al., 2008; Blanchard et al., 2009; Dickson et al., 2015). However, the lack of *Tmod2* seems to be protective, potentially due to modifications in intrinsic and synaptic properties of reward regions that regulate reward learning (Kauer and Malenka, 2007; Kourrich et al., 2015). In animal models, preexisting excitability or optogenetic stimulation of the prefrontal cortex and deep brain stimulation of the accumbens shell but not the core attenuate cocaine-induced behaviors (Chang et al., 1997; Sun and Rebec, 2006; Chen et al., 2013; Vassoler et al., 2013). It is intriguing to speculate that the hyperexcitability of the prefrontal cortex and ventral striatum neurons that we observed in *Tmod2* mutants may actively resist the cocaine-induced depression of these regions, thereby masking the maladaptive behavioral effects of cocaine. Basal and cocaine-induced changes in synaptic properties of accumbens neurons are also perturbed in *Tmod2* KO. Specifically, an elevated basal amplitude of excitatory glutamatergic synapses and unaffected release probability from presynaptic neurons in *Tmod2* KO striatal neurons demonstrate altered the AMPA receptor number or function and the absence of cocaine-induced presynaptic plasticity (Kourrich et al., 2007; Kim et al., 2011). Similarly, accumbens shell neurons exhibit modified, drug-independent inhibitory presynaptic responses that are further amplified by chronic drug exposure. Although drug-induced excitatory synaptic events are well characterized in the nucleus accumbens, little is known about inhibitory synapses and how they respond to repeated cocaine challenge. Previous reports suggest an absence or decrease in the postsynaptic and presynaptic strengthening of inhibitory neurotransmission following cocaine exposure (Kim et al., 2011). Although the available literature is biased toward the role of *TMOD2* in the postsynaptic dendritic

compartment, our study clearly shows presynaptic effects on neurotransmission that leads to frequency modulation in excitatory and inhibitory synapses. Interestingly, the acute locomotor response to cocaine is not affected in *Tmod2* KO and argues that the basal ganglia circuit, which regulates drug-induced locomotor activation, is not perturbed (Bateup et al., 2010).

Recent human GWAS studies has linked *Tmod2* variants with intellectual disability (Davies et al., 2018) and intelligence (Hill et al., 2019) and has suggested an important role of *Tmod2* gene in influencing normal cognitive functions in human. Operant learning, as accessed by operant cocaine and food self-administration, is a form of associative learning that is dependent on various brain regions including the nucleus accumbens and hippocampus (Day et al., 2007; Brincat and Miller, 2015). *Tmod2* KO shows deficits in associative learning with delayed performance in operant conditioning, but no deficits in motor learning as determined by the rotarod assay. In addition, KO mice show enhanced nonassociative learning which is demonstrated by enhanced habituation of hyperactivity and anxiety measures in the open field. Thus, there is specificity in the type of learning that is regulated by *Tmod2*. Sensitivity to natural reward is the unexplored aspect of this study. However, given that *Tmod2* could successfully respond to an intermediate concentration (4% sucrose) of natural reward in a two-bottle sucrose preference assay, we can conclude that failure to acquire cocaine in an IVSA paradigm was not due to a general deficit in the reward-sensing neural circuit. Another facet of learning deficit that remains unexplored in this study is whether the negative reinforcement-based self-medication triggered by aversive environmental conditions is compromised in *Tmod2* mutants leading to failure in drug acquisition and intake in the IVSA paradigm (Fouyssac et al., 2021).

Since *Tmod2* regulates actin function (Gray et al., 2017), we tested the mutants for structural anomalies of the brain using MRI. We found a ~9% reduction of total brain volume, with 60% of the structures evaluated across the brain affected. However, after correction for differences in whole brain size (accounting for global volume differences), a smaller number of key structural differences were isolated: (1) decreased volumes across a number of regions notably including white matter structures and the thalamus and (2) volume increases over a number of regions including the basal forebrain and the nucleus accumbens. Comparable human MRI studies of addiction include reports of a number of morphological or microstructural changes related to the regions identified in the *Tmod2* KO mice. For example, decreased fractional anisotropy indicates abnormality in the white matter and has been reported in the frontal white matter (Lim et al., 2008) and in the corpus callosum (Moeller et al., 2005) of cocaine-dependent individuals. The thalamus, frequently linked to addiction, has also been studied frequently, but morphological findings are inconsistent, with volume increases, decreases, or no change reported (Garza-Villarreal et al., 2017). More consistent findings have been observed in the nucleus accumbens, where decreased volumes have been identified in crack cocaine users (Garza-Villarreal et al., 2017) and increased volumes are associated with the duration of abstinence (from alcohol, cannabis, and/or cocaine) in former users (Korponay et al., 2017). It remains unclear in these human studies, however, whether the morphological findings predate or emerge after substance use. Given that the *Tmod2* KO mice evaluated by MRI in this study were cocaine naive, it is difficult to relate the morphological findings directly to human observations. Although we did not perform measurements of fractional anisotropy in this work,

the smaller white matter volumes in the *Tmod2* KO mice may be inconsistent with changes observed in humans, in which microstructural changes evident in fractional anisotropy were linked with drug use. On the other hand, the larger relative volume of the nucleus accumbens in *Tmod2* KO mice, and the corresponding reduced IVSA, appears consistent with the expectations from human findings that an increased accumbens volume would be associated with a reduced addiction phenotype (Korponay et al., 2017). Of course, the morphological changes observed in the *Tmod2* KO mice represent the net result of a complex developmental process, including influences of altered synapse formation and/or function. Thus, like the behavioral phenotype, morphological changes may be secondary to other dysfunctional cellular processes. The complex interplay of these interactions is an ongoing topic in neurodevelopmental research.

The neuronal restriction of *Tmod2* expression combined with its functional role in regulating cocaine intake could potentially be harnessed as a pharmacotherapy for addiction-related behaviors. Recently, nonmuscle myosin IIB that regulates synaptic actin polymerization has been proposed as a potential therapeutic target for the treatment of methamphetamine addiction, but has been found to be ineffective against cocaine- or morphine-associated contextual memory (Young et al., 2016; Briggs et al., 2017, 2018). Our behavioral and electrophysiology data argue that *Tmod2* has a protective role in transition to addiction, perhaps through regulation of basal or drug-induced balance of excitatory and inhibitory networks. The impairment in cocaine-based reward learning, but no deficits in motor learning or non-associative learning, indicates specificity of TMOD2 function. Future studies with cell-type and temporally specific *Tmod2* knock-outs are required to tease apart this specificity and to address the developmental role of TMOD2 in the reward circuit. The current findings combined with our previous results (Kumar et al., 2013) emphasize the advantage of unbiased forward genetic approaches to studying addiction-related behavior.

References

- Agrawal HC, Davis JM, Himwich WA (1968) Developmental changes in mouse brain: weight, water content and free amino acids. *J Neurochem* 15:917–923.
- Areal LB, Hamilton A, Martins-Silva C, Pires RGW, Ferguson SSG (2019) Neuronal scaffolding protein spinophilin is integral for cocaine-induced behavioral sensitization and ERK1/2 activation. *Mol Brain* 12:15.
- Badiani A, Robinson TE (2004) Drug-induced neurobehavioral plasticity: the role of environmental context. *Behav Pharmacol* 15:327–339.
- Bailey SA, Zidell RH, Perry RW (2004) Relationships between organ weight and body/brain weight in the rat: what is the best analytical endpoint? *Toxicol Pathol* 32:448–466.
- Ball SA, Kranzler HR, Tennen H, Poling JC, Rounsaville BJ (1998) Personality disorder and dimension differences between type A and type B substance abusers. *J Pers Disord* 12:1–12.
- Bateup HS, Santini E, Shen W, Birnbaum S, Valjent E, Surmeier DJ, Fisone G, Nestler EJ, Greengard P (2010) Distinct subclasses of medium spiny neurons differentially regulate striatal motor behaviors. *Proc Natl Acad Sci U S A* 107:14845–14850.
- Belin D, Mar AC, Dalley JW, Robbins TW, Everitt BJ (2008) High impulsivity predicts the switch to compulsive cocaine taking. *Science* 320:1352–1355.
- Belin D, Berson N, Balado E, Piazza PV, Deroche-Gamonet V (2011) High-novelty-preference rats are predisposed to compulsive cocaine self-administration. *Neuropsychopharmacology* 36:569–579.
- Belin-Rauscent A, Fouyssac M, Bonci A, Belin D (2016) How preclinical models evolved to resemble the diagnostic criteria of drug addiction. *Biol Psychiatry* 79:39–46.
- Benavides DR, Quinn JJ, Zhong P, Hawasli AH, DiLeone RJ, Kansy JW, Olausson P, Yan Z, Taylor JR, Bibb JA (2007) Cdk5 modulates cocaine reward, motivation, and striatal neuron excitability. *J Neurosci* 27:12967–12976.
- Benjamini Y, Hochberg Y (1995) Controlling the false discovery rate: a practical and powerful approach to multiple testing. *J R Stat Soc Series B Methodol* 57:289–300.
- Benuck M, Lajtha A, Reith ME (1987) Pharmacokinetics of systemically administered cocaine and locomotor stimulation in mice. *J Pharmacol Exp Ther* 243:144–149.
- Blanchard MM, Mendelsohn D, Stamp JA (2009) The HR/LR model: further evidence as an animal model of sensation seeking. *Neurosci Biobehav Rev* 33:1145–1154.
- Bolivar VJ (2009) Intrasession and intersession habituation in mice: from inbred strain variability to linkage analysis. *Neurobiol Learn Mem* 92:206–214.
- Brady KT, Haynes LF, Hartwell KJ, Killeen TK (2013) Substance use disorders and anxiety: a treatment challenge for social workers. *Soc Work Public Health* 28:407–423.
- Briggs SB, Blouin AM, Young EJ, Rumbaugh G, Miller CA (2017) Memory disrupting effects of nonmuscle myosin II inhibition depend on the class of abused drug and brain region. *Learn Mem* 24:70–75.
- Briggs SB, Hafenbreidel M, Young EJ, Rumbaugh G, Miller CA (2018) The role of nonmuscle myosin II in polydrug memories and memory reconsolidation. *Learn Mem* 25:391–398.
- Brincat SL, Miller EK (2015) Frequency-specific hippocampal-prefrontal interactions during associative learning. *Nat Neurosci* 18:576–581.
- Cahill ME, Walker DM, Gancarz AM, Wang ZJ, Lardner CK, Bagot RC, Neve RL, Dietz DM, Nestler EJ (2017) The dendritic spine morphogenic effects of repeated cocaine use occur through the regulation of serum response factor signaling. *Mol Psychiatry* 23:1474.
- Chang JY, Zhang L, Janak PH, Woodward DJ (1997) Neuronal responses in prefrontal cortex and nucleus accumbens during heroin self-administration in freely moving rats. *Brain Res* 754:12–20.
- Chen BT, Yau H-J, Hatch C, Kusumoto-Yoshida I, Cho SL, Hopf FW, Bonci A (2013) Rescuing cocaine-induced prefrontal cortex hypoactivity prevents compulsive cocaine seeking. *Nature* 496:359–362.
- Cox PR, Zoghbi HY (2000) Sequencing, expression analysis, and mapping of three unique human tropomodulin genes and their mouse orthologs. *Genomics* 63:97–107.
- Cox PR, Fowler V, Xu B, Sweatt JD, Paylor R, Zoghbi HY (2003) Mice lacking tropomodulin-2 show enhanced long-term potentiation, hyperactivity, and deficits in learning and memory. *Mol Cell Neurosci* 23:1–12.
- Davies G, et al. (2018) Study of 300,486 individuals identifies 148 independent genetic loci influencing general cognitive function. *Nat Commun* 9:2098.
- Davis BA, Clinton SM, Akil H, Becker JB (2008) The effects of novelty-seeking phenotypes and sex differences on acquisition of cocaine self-administration in selectively bred high-responder and low-responder rats. *Pharmacol Biochem Behav* 90:331–338.
- Day JJ, Roitman MF, Wightman RM, Carelli RM (2007) Associative learning mediates dynamic shifts in dopamine signaling in the nucleus accumbens. *Nat Neurosci* 10:1020–1028.
- de Guzman AE, Wong MD, Gleave JA, Nieman BJ (2016) Variations in post-perfusion immersion fixation and storage alter MRI measurements of mouse brain morphometry. *Neuroimage* 142:687–695.
- Deller T, et al. (2003) Synaptopodin-deficient mice lack a spine apparatus and show deficits in synaptic plasticity. *Proc Natl Acad Sci U S A* 100:10494–10499.
- Dellu F, Piazza PV, Mayo W, Le Moal M, Simon H (1996) Novelty-seeking in rats—biobehavioral characteristics and possible relationship with the sensation-seeking trait in man. *Neuropsychobiology* 34:136–145.
- Dickson PE, Rogers TD, Lester DB, Miller MM, Matta SG, Chesler EJ, Goldowitz D, Blaha CD, Mittleman G (2011) Genotype-dependent effects of adolescent nicotine exposure on dopamine functional dynamics in the nucleus accumbens shell in male and female mice: a potential mechanism underlying the gateway effect of nicotine. *Psychopharmacology* 215:631–642.
- Dickson PE, Ndukum J, Wilcox T, Clark J, Roy B, Zhang L, Li Y, Lin D-T, Chesler EJ (2015) Association of novelty-related behaviors and intravenous cocaine self-administration in diversity outbred mice. *Psychopharmacology (Berl)* 232:1011–1024.
- Dilleen R, Pelloux Y, Mar AC, Molander A, Robbins TW, Everitt BJ, Dalley JW, Belin D (2012) High anxiety is a predisposing endophenotype for loss of control over cocaine, but not heroin, self-administration in rats. *Psychopharmacology (Berl)* 222:89–97.
- Dorr AE, Lerch JP, Spring S, Kabani N, Henkelman RM (2008) High resolution three-dimensional brain atlas using an average magnetic resonance image of 40 adult C57Bl/6J mice. *Neuroimage* 42:60–69.

- Dos Santos M, Salery M, Forget B, Garcia Perez MA, Betuing S, Boudier T, Vanhoutte P, Caboche J, Heck N (2017) Rapid synaptogenesis in the nucleus accumbens is induced by a single cocaine administration and stabilized by mitogen-activated protein kinase interacting kinase-1 activity. *Biol Psychiatry* 82:806–818.
- Eagle AL, Gajewski PA, Yang M, Kechner ME, Al Masraf BS, Kennedy PJ, Wang H, Mazei-Robison MS, Robison AJ (2015) Experience-dependent induction of hippocampal Δ FosB controls learning. *J Neurosci* 35:13773–13783.
- Feng J, Yan Z, Ferreira A, Tomizawa K, Liauw JA, Zhuo M, Allen PB, Ouimet CC, Greengard P (2000) Spinophilin regulates the formation and function of dendritic spines. *Proc Natl Acad Sci U S A* 97:9287–9292.
- Fischer RS, Fowler VM (2003) Tropomodulins: life at the slow end. *Trends Cell Biol* 13:593–601.
- Fouyssac M, et al. (2021) Environment-dependent behavioral traits and experiential factors shape addiction vulnerability. *Eur J Neurosci* 53:1794–1808.
- Franques P, Auriacombe M, Piquemal E, Verger M, Brisseau-Gimenez S, Grabot D, Tignol J (2003) Sensation seeking as a common factor in opioid dependent subjects and high risk sport practicing subjects: a cross-sectional study. *Drug Alcohol Depend* 69:121–126.
- Friedel M, van Eede MC, Pipitone J, Chakravarty MM, Lerch JP (2014) Pypdiper: a flexible toolkit for constructing novel registration pipelines. *Front Neuroinform* 8:67.
- Furukawa K, Fu W, Li Y, Witke W, Kwiatkowski DJ, Mattson MP (1997) The actin-severing protein gelsolin modulates calcium channel and NMDA receptor activities and vulnerability to excitotoxicity in hippocampal neurons. *J Neurosci* 17:8178–8186.
- Garza-Villarreal EA, et al. (2017) The effect of crack cocaine addiction and age on the microstructure and morphology of the human striatum and thalamus using shape analysis and fast diffusion kurtosis imaging. *Transl Psychiatry* 7:e1122.
- Gray KT, Suchowerska AK, Bland T, Colpan M, Wayman G, Fath T, Kostyukova AS (2016) Tropomodulin isoforms utilize specific binding functions to modulate dendrite development. *Cytoskeleton (Hoboken)* 73:316–328.
- Gray KT, Kostyukova AS, Fath T (2017) Actin regulation by tropomodulin and tropomyosin in neuronal morphogenesis and function. *Mol Cell Neurosci* 84:48–57.
- Grueter BA, Rothwell PE, Malenka RC (2012) Integrating synaptic plasticity and striatal circuit function in addiction. *Curr Opin Neurobiol* 22:545–551.
- Gu Z, Fonseca V, Hai C (2013) Nicotinic acetylcholine receptor mediates nicotine-induced actin cytoskeletal remodeling and extracellular matrix degradation by vascular smooth muscle cells. *Vascu Pharmacol* 58:87–97.
- Hascöet M, Bourin M, Nic Dhonnchadha BA (2001) The mouse light-dark paradigm: a review. *Prog Neuropsychopharmacol Biol Psychiatry* 25:141–166.
- Hill WD, Marioni RE, Maghazian O, Ritchie SJ, Hagensars SP, McIntosh AM, Gale CR, Davies G, Deary IJ (2019) A combined analysis of genetically correlated traits identifies 187 loci and a role for neurogenesis and myelination in intelligence. *Mol Psychiatry* 24:169–181.
- Hu Z, Yu D, Gu QH, Yang Y, Tu K, Zhu J, Li Z (2014) miR-191 and miR-135 are required for long-lasting spine remodeling associated with synaptic long-term depression. *Nat Commun* 5:3263.
- Ishikawa M, Otaka M, Neumann PA, Wang Z, Cook JM, Schluter OM, Dong Y, Huang YH (2013) Exposure to cocaine regulates inhibitory synaptic transmission from the ventral tegmental area to the nucleus accumbens. *J Physiol* 591:4827–4841.
- Iwazaki T, McGregor IS, Matsumoto I (2006) Protein expression profile in the striatum of acute methamphetamine-treated rats. *Brain Res* 1097:19–25.
- Jewett KA, Lee KY, Egleman DE, Soriano S, Tsai N-P (2018) Dysregulation and restoration of homeostatic network plasticity in fragile X syndrome mice. *Neuropharmacology* 138:182–192.
- Kasanetz F, Deroche-Gamonet V, Berson N, Balado E, Lafourcade M, Manzoni O, Piazza PV (2010) Transition to addiction is associated with a persistent impairment in synaptic plasticity. *Science* 328:1709–1712.
- Kasanetz F, Lafourcade M, Deroche-Gamonet V, Revest J-M, Berson N, Balado E, Fiancette J-F, Renault P, Piazza P-V, Manzoni OJ (2013) Prefrontal synaptic markers of cocaine addiction-like behavior in rats. *Mol Psychiatry* 18:729–737.
- Kauer JA, Malenka RC (2007) Synaptic plasticity and addiction. *Nat Rev Neurosci* 8:844–858.
- Kilman V, van Rossum MCW, Turrigiano GG (2002) Activity deprivation reduces miniature IPSC amplitude by decreasing the number of postsynaptic GABA(A) receptors clustered at neocortical synapses. *J Neurosci* 22:1328–1337.
- Kim MH, et al. (2009) Enhanced NMDA receptor-mediated synaptic transmission, enhanced long-term potentiation, and impaired learning and memory in mice lacking IRSp53. *J Neurosci* 29:1586–1595.
- Kim J, Park B-H, Lee JH, Park SK, Kim J-H (2011) Cell type-specific alterations in the nucleus accumbens by repeated exposures to cocaine. *Biol Psychiatry* 69:1026–1034.
- Kiraly DD, Ma XM, Mazzone CM, Xin X, Mains RE, Eipper BA (2010) Behavioral and morphological responses to cocaine require kalirin7. *Biol Psychiatry* 68:249–255.
- Korponay C, Kosson DS, Decety J, Kiehl KA, Koenigs M (2017) Brain volume correlates with duration of abstinence from substance abuse in a region-specific and substance-specific manner. *Biol Psychiatry Cogn Neurosci Neuroimaging* 2:626–635.
- Kourrich S, Rothwell PE, Klug JR, Thomas MJ (2007) Cocaine experience controls bidirectional synaptic plasticity in the nucleus accumbens. *J Neurosci* 27:7921–7928.
- Kourrich S, Calu DJ, Bonci A (2015) Intrinsic plasticity: an emerging player in addiction. *Nat Rev Neurosci* 16:173–184.
- Kumar V, et al. (2013) C57BL/6N mutation in cytoplasmic FMRP interacting protein 2 regulates cocaine response. *Science* 342:1508–1512.
- Kumar V, Kim K, Joseph C, Thomas LC, Hong H, Takahashi JS (2011) Second-generation high-throughput forward genetic screen in mice to isolate subtle behavioral mutants. *Proc Natl Acad Sci U S A* 108(Suppl 3):15557–15564.
- Lerch JP, Gazdzinski L, Germann J, Sled JG, Henkelman RM, Nieman BJ (2012) Wanted dead or alive? The tradeoff between in-vivo versus ex-vivo MR brain imaging in the mouse. *Front Neuroinform* 6:6.
- Lesscher HM, Houthuijzen JM, Groot Koerkamp MJ, Holstege FC, Vanderschuren LJ (2012) Amygdala 14-3-3zeta as a novel modulator of escalating alcohol intake in mice. *PLoS One* 7:e37999.
- Lever C, Burton S, O’Keefe J (2006) Rearing on hind legs, environmental novelty, and the hippocampal formation. *Rev Neurosci* 17:111–133.
- Li CY, Mao X, Wei L (2008) Genes and (common) pathways underlying drug addiction. *PLoS Comput Biol* 4:e2.
- Li G, Wang Y, Yan M, Xu Y, Song X, Li Q, Zhang J, Ma H, Wu Y (2015) Inhibition of actin polymerization in the NAc shell inhibits morphine-induced CPP by disrupting its reconsolidation. *Sci Rep* 5:16283.
- Li Z, Chen Z, Fan G, Li A, Yuan J, Xu T (2018) Cell-type-specific afferent innervation of the nucleus accumbens core and shell. *Front Neuroanat* 12:84.
- Lim KO, Wozniak JR, Mueller BA, Franc DT, Specker SM, Rodriguez CP, Silverman AB, Rotrosen JP (2008) Brain macrostructural and microstructural abnormalities in cocaine dependence. *Drug Alcohol Depend* 92:164–172.
- Lin WH, Nebhan CA, Anderson BR, Webb DJ (2010) Vasodilator-stimulated phosphoprotein (VASP) induces actin assembly in dendritic spines to promote their development and potentiate synaptic strength. *J Biol Chem* 285:36010–36020.
- Lüscher C, Malenka RC (2011) Drug-evoked synaptic plasticity in addiction: from molecular changes to circuit remodeling. *Neuron* 69:650–663.
- Ly C, et al. (2018) Psychedelics promote structural and functional neural plasticity. *Cell Rep* 23:3170–3182.
- Malenka RC, Nicoll RA (1999) Long-term potentiation—a decade of progress? *Science* 285:1870–1874.
- Mark A, Sussman SS (1994) <Neural tropomodulin-developmental expression and effect of seizure activity_Sussman1994.pdf>.
- Mello NK, Negus SS (1996) Preclinical evaluation of pharmacotherapies for treatment of cocaine and opioid abuse using drug self-administration procedures. *Neuropsychopharmacology* 14:375–424.
- Miller EC, Zhang L, Dummer BW, Cariveau DR, Loh H, Law PY, Liao D (2012) Differential modulation of drug-induced structural and functional plasticity of dendritic spines. *Mol Pharmacol* 82:333–343.
- Moeller FG, Hasan KM, Steinberg JL, Kramer LA, Dougherty DM, Santos RM, Valdes I, Swann AC, Barratt ES, Narayana PA (2005) Reduced anterior corpus callosum white matter integrity is related to increased impulsivity and reduced discriminability in cocaine-dependent subjects: diffusion tensor imaging. *Neuropsychopharmacology* 30:610–617.
- Molander AC, et al. (2011) High impulsivity predicting vulnerability to cocaine addiction in rats: some relationship with novelty preference but

- not novelty reactivity, anxiety or stress. *Psychopharmacology (Berl)* 215:721–731.
- Norrholm SD, Bibb JA, Nestler EJ, Ouimet CC, Taylor JR, Greengard P (2003) Cocaine-induced proliferation of dendritic spines in nucleus accumbens is dependent on the activity of cyclin-dependent kinase-5. *Neuroscience* 116:19–22.
- Offenhauser N, et al. (2006) Increased ethanol resistance and consumption in *Eps8* knockout mice correlates with altered actin dynamics. *Cell* 127:213–226.
- Ojelade SA, et al. (2015) *Rsu1* regulates ethanol consumption in *Drosophila* and humans. *Proc Natl Acad Sci U S A* 112:E4085.
- Oliver RJ, Brigman JL, Bolognani F, Allan AM, Neisewander JL, Perrone-Bizzozero NI (2018) Neuronal RNA-binding protein HuD regulates addiction-related gene expression and behavior. *Genes Brain Behav* 17:e12454.
- Omotade OF, Rui Y, Lei W, Yu K, Hartzell HC, Fowler VM, Zheng JQ (2018) Tropomodulin isoform-specific regulation of dendrite development and synapse formation. *J Neurosci* 38:10271–10285.
- Parikshak NN, Gandal MJ, Geschwind DH (2015) Systems biology and gene networks in neurodevelopmental and neurodegenerative disorders. *Nat Rev Genet* 16:441–458.
- Phillips TJ (1997) Behavior genetics of drug sensitization. *Crit Rev Neurobiol* 11:21–33.
- Pilo Boyl P, et al. (2007) *Profilin2* contributes to synaptic vesicle exocytosis, neuronal excitability, and novelty-seeking behavior. *EMBO J* 26:2991–3002.
- Polimanti R, Meda SA, Pearlson GD, Zhao H, Sherva R, Farrer LA, Kranzler HR, Gelernter J (2017) *S100a10* identified in a genome-wide gene x cannabis dependence interaction analysis of risky sexual behaviours. *J Psychiatry Neurosci* 42:252–261.
- Pulipparacharuvil S, et al. (2008) Cocaine regulates MEF2 to control synaptic and behavioral plasticity. *Neuron* 59:621–633.
- Ragu Varman D, Subler MA, Windle JJ, Jayanthi LD, Ramamoorthy S (2021) Novelty-induced hyperactivity and suppressed cocaine induced locomotor activation in mice lacking threonine 53 phosphorylation of dopamine transporter. *Behav Brain Res* 408:113267.
- Robinson TE, Berridge KC (2003) Addiction. *Annu Rev Psychol* 54:25–53.
- Robinson TE, Kolb B (1999) Alterations in the morphology of dendrites and dendritic spines in the nucleus accumbens and prefrontal cortex following repeated treatment with amphetamine or cocaine. *Eur J Neurosci* 11:1598–1604.
- Robinson TE, Kolb B (2004) Structural plasticity associated with exposure to drugs of abuse. *Neuropharmacology* 47(Suppl 1):33–46.
- Rothenfluh A, Cowan CW (2013) Emerging roles of actin cytoskeleton regulating enzymes in drug addiction: actin or reactin? *Curr Opin Neurobiol* 23:507–512.
- Russo SJ, Dietz DM, Dumitriu D, Morrison JH, Malenka RC, Nestler EJ (2010) The addicted synapse: mechanisms of synaptic and structural plasticity in nucleus accumbens. *Trends Neurosci* 33:267–276.
- Ryder MI (1994) Nicotine effects on neutrophil F-actin formation and calcium release: implications for tobacco use and pulmonary diseases. *Exp Lung Res* 20:283–296.
- Sanchis-Segura C, Spanagel R (2006) Behavioural assessment of drug reinforcement and addictive features in rodents: an overview. *Addict Biol* 11:2–38.
- Soderling SH, Guire ES, Kaech S, White J, Zhang F, Schutz K, Langeberg LK, Banker G, Raber J, Scott JD (2007) A WAVE-1 and WRP signaling complex regulates spine density, synaptic plasticity, and memory. *J Neurosci* 27:355–365.
- Spencer Noakes TL, Henkelman RM, Nieman BJ (2017) Partitioning k-space for cylindrical three-dimensional rapid acquisition with relaxation enhancement imaging in the mouse brain. *NMR Biomed* 30.
- Srinivasan K, et al. (2016) Untangling the brain's neuroinflammatory and neurodegenerative transcriptional responses. *Nat Commun* 7:11295.
- Star EN, Kwiatkowski DJ, Murthy VN (2002) Rapid turnover of actin in dendritic spines and its regulation by activity. *Nat Neurosci* 5:239–246.
- Steketee JD, Kalivas PW (2011) Drug wanting: behavioral sensitization and relapse to drug-seeking behavior. *Pharmacol Rev* 63:348–365.
- Sun W, Rebec GV (2006) Repeated cocaine self-administration alters processing of cocaine-related information in rat prefrontal cortex. *J Neurosci* 26:8004–8008.
- Tapocik JD, Luu TV, Mayo CL, Wang BD, Doyle E, Lee AD, Lee NH, Elmer GI (2013) Neuroplasticity, axonal guidance and micro-RNA genes are associated with morphine self-administration behavior. *Addict Biol* 18:480–495.
- Thomsen M, Caine SB (2007) Intravenous drug self-administration in mice: practical considerations. *Behav Genet* 37:101–118.
- Toda S, Shen HW, Peters J, Cagle S, Kalivas PW (2006) Cocaine increases actin cycling: effects in the reinstatement model of drug seeking. *J Neurosci* 26:1579–1587.
- Tolliver BK, Carney JM (1994) Sensitization to stereotypy in DBA/2J but not C57BL/6J mice with repeated cocaine. *Pharmacol Biochem Behav* 48:169–173.
- Torre D, Lachmann A, Ma'ayan A (2018) Biojupies: automated generation of interactive notebooks for RNA-seq data analysis in the cloud. *Cell Syst* 7:556–561.e3.
- Tsai NP, Wilkerson JR, Guo W, Maksimova MA, DeMartino GN, Cowan CW, Huber KM (2012) Multiple autism-linked genes mediate synapse elimination via proteasomal degradation of a synaptic scaffold PSD-95. *Cell* 151:1581–1594.
- Turner BD, Kashima DT, Manz KM, Grueter CA, Grueter BA (2018) Synaptic plasticity in the nucleus accumbens: lessons learned from experience. *ACS Chem Neurosci* 9:2114–2126.
- Vanderschuren LJ, Kalivas PW (2000) Alterations in dopaminergic and glutamatergic transmission in the induction and expression of behavioral sensitization: a critical review of preclinical studies. *Psychopharmacology (Berl)* 151:99–120.
- van Huijstee AN, Mansvelder HD (2015) Glutamatergic synaptic plasticity in the mesocorticolimbic system in addiction. *Front Cell Neurosci* 8:466.
- Vassoler FM, White SL, Hopkins TJ, Guercio LA, Espallergues J, Berton O, Schmidt HD, Pierce RC (2013) Deep brain stimulation of the nucleus accumbens shell attenuates cocaine reinstatement through local and antidromic activation. *J Neurosci* 33:14446–14454.
- Volkow ND, Morales M (2015) The brain on drugs: from reward to addiction. *Cell* 162:712–725.
- Volkow ND, Michaelides M, Baler R (2019) The neuroscience of drug reward and addiction. *Physiol Rev* 99:2115–2140.
- Watakabe A, Kobayashi R, Helfman DM (1996) N-tropomodulin: a novel isoform of tropomodulin identified as the major binding protein to brain tropomyosin. *J Cell Sci* 109(Pt 9):2299–2310.
- Weber A, Pennise CR, Fowler VM (1999) Tropomodulin increases the critical concentration of barbed end-capped actin filaments by converting ADP.P(i)-actin to ADP-actin at all pointed filament ends. *J Biol Chem* 274:34637–34645.
- Wolf ME (2016) Synaptic mechanisms underlying persistent cocaine craving. *Nat Rev Neurosci* 17:351–365.
- Wu LJ, Ren M, Wang H, Kim SS, Cao X, Zhuo M (2008) Neurabin contributes to hippocampal long-term potentiation and contextual fear memory. *PLoS One* 3:e1407.
- Yamashiro S, Speicher KD, Speicher DW, Fowler VM (2010) Mammalian tropomodulins nucleate actin polymerization via their actin monomer binding and filament pointed end-capping activities. *J Biol Chem* 285:33265–33280.
- Young EJ, Briggs SB, Miller CA (2015) The actin cytoskeleton as a therapeutic target for the prevention of relapse to methamphetamine use. *CNS Neurol Disord Drug Targets* 14:731–737.
- Young EJ, Blouin AM, Briggs SB, Sillivan SE, Lin L, Cameron MD, Rumbaugh G, Miller CA (2016) Nonmuscle myosin IIB as a therapeutic target for the prevention of relapse to methamphetamine use. *Mol Psychiatry* 21:615–623.
- Zhang ZW (2004) Maturation of layer V pyramidal neurons in the rat prefrontal cortex: intrinsic properties and synaptic function. *J Neurophysiol* 91:1171–1182.
- Zhang ZW, Arsenault D (2005) Gain modulation by serotonin in pyramidal neurones of the rat prefrontal cortex. *J Physiol* 566:379–394.
- Zhang F, Chen L, Liu C, Qiu P, Wang A, Li L, Wang H (2013) Up-regulation of protein tyrosine nitration in methamphetamine-induced neurotoxicity through DDAH/ADMA/NOS pathway. *Neurochem Int* 62:1055–1064.
- Zhang W, Peterson M, Beyer B, Frankel WN, Zhang Z (2014) Loss of MeCP2 from forebrain excitatory neurons leads to cortical hyperexcitation and seizures. *J Neurosci* 34:2754–2763.
- Zhu L, Li J, Dong N, Guan F, Liu Y, Ma D, Goh EL, Chen T (2016) mRNA changes in nucleus accumbens related to methamphetamine addiction in mice. *Sci Rep* 6:36993.